Foraging on host synthesized metabolites enables the bacterial symbiont *Snodgrassella alvi* to colonize the honey bee gut

Andrew Quinn[1,A], Yassine El Chazli[1,A], Stéphane Escrig[2], Jean Daraspe[3], Nicolas Neuschwander[1], Aoife McNally[1], Christel Genoud[3], Anders Meibom[2,4], Philipp Engel[1,*]

[1] Department of Fundamental Microbiology, University of Lausanne, Lausanne, Switzerland

[2]Laboratory of Biological Geochemistry, Ecole Polytechnique Fédérale de Lausanne (EPFL), Lausanne, Switzerland.

[3] Electron Microscopy Facility, University of Lausanne, Lausanne, Switzerland

[4] Center for Advanced Surface Analysis, Institute of Earth Sciences, University of Lausanne, Lausanne, Switzerland

[A] Equally contributing first authors

* Corresponding author: phillipp.engel@unil.ch

Keywords

Microbiome, microbiota, insect, symbiosis, metabolomics, NanoSIMS isotope-tracing, gnotobiotic, mass spectrometry, proteobacteria.

Summary

Dietary nutrients and microbial cross-feeding allow diverse bacteria to colonize the animal gut. Less is known about the role of host-derived nutrients in enabling gut bacterial colonization. We examined metabolic interactions within the evolutionary ancient symbiosis between the honey bee (*Apis mellifera*) and the core gut microbiota member *Snodgrassella alvi*. This Betaproteobacteria is incapable of metabolizing saccharides, yet colonizes the honey bee gut in the presence of only a sugar diet. Using comparative metabolomics, ^{13}C tracers, and Nanoscale secondary ion mass spectrometry (NanoSIMS), we show *in vivo* that *S. alvi* grows on host-derived organic acids, including citrate, glycerate and 3-hydroxy-3-methylglutarate which are actively secreted by the host into the gut lumen. *S. alvi* additionally modulates tryptophan metabolism in the gut by converting kynurenine to anthranilate. These results suggest that *S. alvi* is adapted to a specific metabolic niche in the gut that depends on host-derived nutritional resources.

33 # Introduction

34 Gut bacteria and their hosts typically engage in mutualistic interactions. Metabolic exchange from the
35 gut microbiota to the host is vital for uptake of essential nutrients, gut health and immune system
36 function [1]. In turn, bacteria profit from a stable niche environment and frequent supply of exogenous
37 food. The role of host secreted metabolites that benefit bacteria in the gut is less well understood. Such
38 metabolic exchange is difficult to identify due to the overwhelming contributions of the diet and
39 microbial products towards gut metabolites.

40 Deciphering the extent to which host metabolite secretion drives microbial colonization of native
41 symbionts is aided by a simple, tractable system in which diet and microbiota-derived metabolites can
42 be tightly controlled. The Western honey bee (*Apis mellifera*) provides such a system: Its gut microbiota
43 is broadly stable and composed of only 8-10 genera [2,3] many of which have longstanding evolutionary
44 associations with their host that date back to the emergence of social bees >80 mya [4-6]. Bacteria of these
45 genera are culturable and can be inoculated individually or as defined communities into gnotobiotic
46 bees [7]. Furthermore, while the typical honey bee diet features a rich mixture of compounds found in
47 nectar and pollen, bees can survive for extended periods on pure sugar water diets [8].

48 Most members of the bee gut microbiome are primary fermenters, possessing a broad range of
49 carbohydrate degradation enzymes that enable them to utilize hemicellulose, pectin, starch, or
50 glycosides found in pollen [3,9]. A notable exception is the Betaproteobacteria *Snodgrassella alvi*. It
51 colonizes the cuticular surfaces of the ileum in the hindgut and displays a markedly different metabolism
52 [10,11]. Lacking a functional glycolysis pathway, *S. alvi* profits from acids in the gut, generating energy
53 from an aerobic TCA cycle, and biomass through gluconeogenesis. Fermentation by other microbial
54 members has been proposed as the primary source of short chain fatty acids (SCFAs) consumed by *S.*
55 *alvi*. In particular, bacteria of the Gammaproteobacterial genus *Gilliamella* are likely mutualistic
56 partners for metabolic crosstalk, as they co-localize with *S. alvi* within biofilms attached to the cuticular
57 surface in the ileum and share complementary metabolic capabilities [10]. Experimental evidence from *in*
58 *vitro* growth experiments bolstered this hypothesis, showing that *S. alvi* grows on the spent media of

59 *Gilliamella,* while consuming numerous products of *Gilliamella's* metabolism, such as succinate and
60 pyruvate [12].

61 Although a strong case can be made for niche exploitation through bacterial cross-feeding, this
62 hypothesis does not explain previous results in which *S. alvi* was able to mono-colonize bees fed diets
63 of sugar water and pollen [12]. To better understand the nutrient sources that *S. alvi* exploits, we provided
64 bees a simple (sugar water) or complex (sugar water + pollen) diet and colonized them with *S. alvi*
65 alone, or together with divergent strains of the genus *Gilliamella*. Surprisingly, we found that a simple
66 sugar water diet was sufficient for *S. alvi* to colonize the honey bee gut. Subsequent metabolomics
67 analysis indicated that host-derived carboxylic acids enable *S. alvi* colonization. We validated this
68 hypothesis with a series of experiments to show that (i) these carboxylic acids are synthesized by the
69 host, (ii) *S. alvi* utilizes them for growth, and (iii) the findings hold across a range of divergent
70 *Snodgrassella* strains and species.

71

72 Results

73 *S. alvi* colonizes the honey bee gut in the presence of only sugar in the diet

74 We colonized microbiota-free (MF) honey bees with *S. alvi* (strain wkB2) or a mixture of *Gilliamella*
75 strains (strains wkB1, ESL0169, ESL0182, ESL0297) or with both phylotypes together, and provided
76 a diet composed of only sterile-filtered sugar water (sucrose) or sugar water and electron beam-sterilized
77 polyfloral pollen for five days (**Fig. 1A**). Colonization levels of both phylotypes were assessed by qPCR
78 and CFU plating five days post inoculation (**Fig. 1B**, **Fig. S1**). Surprisingly, *S. alvi* colonized at
79 equivalent levels in the guts across all treatment groups, *i.e.*, sugar water in the diet was sufficient to
80 enable *S. alvi* colonization and neither the addition of pollen to the diet nor co-colonization with
81 *Gilliamella* significantly increased *S. alvi* loads (Wilcoxon rank sum test with *S. alvi* (sugar water) as
82 reference group).

83 Importantly, qPCR analysis with universal bacterial and fungal primers showed no or very low levels
84 of amplification in most samples, with the exception of gut samples containing pollen which resulted
85 in relatively high background amplification with the universal bacterial primers as previously reported
86 (**Fig. S1C, D**). Culturing of gut homogenates of MF bees on different media resulted in no microbial
87 growth in any of the tested conditions (see methods). Hence, we can rule out that systematic
88 contaminations with high levels of other microbes facilitated *S. alvi* colonization through cross-feeding
89 in the mono-colonization treatment.

90

91 *S. alvi* depletes organic acids in the honey bee gut

92

93 To search for putative *S. alvi* growth substrates originating from the host, the pollen diet, or *Gilliamella*,
94 we next extracted metabolites from the mid- and hindgut for a subset of the colonized bees and analyzed
95 them via GC-MS. The presence of pollen in the gut significantly increased the abundance of nearly half
96 of the annotated metabolites (125/233) in MF bees (**Fig. S2**). Thus, we compared results between
97 colonized and MF bees only within each dietary treatment. When we examined mono-colonization of
98 *S. alvi* in bees fed with sugar water, we identified multiple carboxylic acids, including citrate, 3-
99 hydroxy-3-methylglutarate (3Hmg), and glycerate that were significantly less abundant than in the MF
100 controls **(Fig. 1C)**. These carboxylic acids, along with others (*e.g.*, 2-ketoisocaproate, alpha-
101 ketoglutarate and malate) were also depleted in *S. alvi* mono-colonized bees that were fed pollen **(Fig.
102 1C)**, despite the substantial differences in the overall metabolite profiles between the two dietary
103 conditions. In contrast, few metabolites were significantly more abundant in *S. alvi* colonized bees
104 relative to MF bees, with only anthranilate, a product of tryptophan metabolism, accumulating in
105 colonized bees of both dietary treatments (**Fig. 1C**).

106 We then fit each metabolite with a mixed linear model to quantify how strongly metabolite changes
107 were influenced (*i.e.*, the fixed effect) by each of the three independent experimental variables (*i.e.*, the
108 presence of *Gilliamella, S. alvi,* or pollen) across the eight experimental conditions, This cross-
109 conditional analysis confirmed that colonization with *S. alvi* resulted in significantly (p-value < 0.05,

110 see Supporting Data, "output.csv") decreased abundances of carboxylic acids, particularly 3Hmg,
111 citrate, malate, fumarate, and glycerate (**Fig. 1D**). We could also infer which metabolites were co-
112 produced, co-consumed, or cross-fed (and in which direction) between the two bacteria (**Fig. 1D**). For
113 example, we found evidence supporting our initial hypothesis of metabolic cross-feeding from
114 *Gilliamella* to *S. alvi* in the form of lactate, pyruvate and other unknown compounds that were more
115 abundant with *Gilliamella* and less abundant with *S. alvi* (**Fig. 1D**, **Fig. S3**). However, we found no
116 evidence of reverse cross-feeding from *S. alvi* to *Gilliamella*. Instead, we found that both species
117 compete for certain metabolites and act synergistically to synthesize others. Competition, or co-
118 consumption, centered on the carboxylic acids, as colonization with *Gilliamella* also led to depletion of
119 citrate and glycerate, and to a lesser extent, malate, and fumarate (**Fig. 1D**, **Fig. S3**). Cooperative
120 synthesis revolved around four metabolites, acetate, succinate, benzoate, and unknown_12.74. Of these,
121 only acetate was also more abundant in mono-colonization (*Gilliamella*) than in MF controls (**Fig. 1D**,
122 **Fig. S3**). Finally, nearly all the metabolites depleted with *S. alvi* colonization were positively affected
123 by pollen, except for citrate, glycerate, acetate, and two unknown compounds, which were unaffected,
124 and urea, whose abundance was negatively correlated with pollen. Taken together, these results show
125 that each of the tested variables impacts nutrient availability and metabolism of *S. alvi*¸ although
126 metabolic cross-feeding and a nutrient rich diet do not lead to increased colonization levels in the gut.

127

128 Host sugar catabolism provides *S. alvi* substrates *in vivo*

129 We next sought to measure host production of carboxylic acids in the guts of MF bees over the first six
130 days post emergence and compare the abundances to what the bee could have extracted from the average
131 amount of pollen consumed (24.3 ± 7.2mg/bee) as estimated based on data collected from the previous
132 experiment (see methods, **Fig. S4** and Table S2). Moreover, in order to rule-out microbial or fungal
133 contamination as a source of these compounds, we rigorously checked once more for live contamination
134 by plating the guts of newly emerged (day zero) and six-day old MF bees on eight different media in
135 three different growth environments (see methods), finding no evidence of live bacterial or fungal
136 contamination (n=8). Even though the bees only consumed sugar water, we found that many gut

137 metabolites, including glycosylamines, sugar alcohols and carboxylic acids, were significantly more
138 abundant six days after emergence (**Fig. S5**). Focusing specifically on the compounds depleted in the
139 presence of *S. alvi*, we found that citrate was most abundant in the gut, with its concentration increasing
140 from 29 ± 14 μmol/mg at Day 0 to 73 ± 34 μmol/mg at Day 6 post emergence. Substantially less citrate,
141 3 ± 2 μmol/mg, was extracted from pollen (**Fig. 2A**). A similar trend was also found for 3Hmg, alpha-
142 ketoglutarate, isocitrate and kynurenine. Of *S. alvi's* putative substrates, only caffeate and lactate were
143 more abundant in pollen than in the bee gut. The increasing abundance of many compounds over six
144 days, as well as their generally low abundance in pollen suggests that active metabolism by the host
145 substantially impacts the gut metabolome, i.e. easily digestible nutrients in the diet are absorbed and
146 metabolized by the bee upstream of the hindgut, while downstream metabolic products are excreted
147 into the hindgut and serve as substrates for *S. alvi*.

148 To corroborate this hypothesis, we fed MF bees for six days with 45% of the dietary sucrose replaced
149 by 100% U-$^{13}C_6$ Glucose. Half of the bees were also provided standard pollen to assess its contribution
150 relative to simple sugars in the synthesis of gut metabolites. We then analyzed the resulting ^{13}C isotopic
151 enrichments in gut metabolites with a focus on those indicated as substrates for *S. alvi*. The carboxylic
152 acids and non-essential amino acids were significantly ^{13}C enriched in the bee gut. In contrast, other
153 compounds, such as kynurenine and essential amino acids did not show any enrichment **(Fig. 2B)**. The
154 lack of isotope labelling indicates that these compounds were not actively synthesized from glucose by
155 adult bees during the first six days post-emergence. Instead, they were either leftover in the gut from
156 the larval development stage or were acquired from the larval diet, such as in the case of essential amino
157 acids and their catabolic products. As expected, the average ^{13}C enrichment levels of most metabolites
158 dropped in bees fed with pollen compared to those fed with sugar water only. The ^{13}C dilution can occur
159 directly from non-labelled metabolites in pollen, as well as indirectly from host metabolism of pollen
160 substrates. However, the average ^{13}C enrichment of carboxylic acids only dropped from 21 ± 6% to 17
161 ± 7%, which serves as further evidence that host metabolism of simple sugars rather than dietary
162 consumption is the predominant source of carboxylic acids in the gut (**Fig. 2B).** We thus conclude from

163 this analysis that the carboxylic acids utilized by *S. alvi* are mostly *de novo* synthesized from sugar
164 metabolism of the host.

165

166 NanoSIMS reveals transfer of host compounds to *S. alvi*

167 While our previous experiments suggested host nutrient foraging by *S. alvi*, the results did not provide
168 direct evidence that *S. alvi* assimilates biomass from these compounds. Therefore, we probed the flow
169 of metabolites from the bee to *S. alvi* using a "pulse-chase" ^{13}C isotope labelling experiment (ILE), and
170 then measured the enrichment within *S. alvi* cells and surrounding host tissue using nanoscale secondary
171 ion mass spectrometry (NanoSIMS) complemented with measurements of metabolite enrichments
172 using GC-MS (**Fig. 3, Dataset S1**). To do so, we enriched newly emerged MF bees in ^{13}C by feeding
173 them 100% U-$^{13}C_6$ glucose for four days after emergence. We then inoculated them with *S. alvi* and
174 waited one day before switching their diet to naturally abundant, 98.9% ^{12}C-Glucose (**Fig. 3A**). This
175 ensured that the largest *S. alvi* population increase, between 24- and 48-hours post-colonization,
176 occurred without a dietary ^{13}C source, but still in a highly ^{13}C labelled environment **(Fig. 3B)**.

177 Accordingly, we measured rapid ^{13}C labelling turnover in *S. alvi* in 18 images coming from two bees
178 (sampled at 48- and 72-hours post-inoculation) in which we could detect bacterial cells **(Fig. 3C, E,**
179 **Dataset S2)**. The ^{13}C enrichment was substantially higher in *S. alvi* cells than in the adjacent host ileum
180 tissue 48 hours after inoculation, but then dropped below the levels of host tissue 72 hours after
181 inoculation (At% = start: 5.56, end: 2.25) **(Fig. 3C)**. In contrast, the ileum tissue displayed a constant
182 ^{13}C enrichment over the course of the experiment (At% = start: 3.31, end: 3.16), whereas the cuticle
183 lining of the gut epithelium was comparatively less enriched initially and continued dropping to almost
184 natural ^{13}C enrichment levels after 72 hours (At% = start: 2.58, end: 1.39) **(Fig. 3C)**.

185 The ^{13}C enrichment of carboxylic acids and host synthesized (non-essential) amino acids in the gut
186 dynamically shifted in response to the $^{13}C/^{12}C$ switch (**Fig. 3D, Dataset S1)**. Initially, they were highly
187 ^{13}C enriched (38 ± 14.7%), but the labelling fell steadily to approximately half the original level (14 ±
188 5.8%) within 48 hours (**Fig. 3D)**. As a control, we found that essential amino acids (non-host

189 synthesized) were not enriched above the level of natural ^{13}C abundance (1.11%) throughout the
190 experiment. Thus, these results show that products of host glucose metabolism are actively used by *S.*
191 *alvi* to build its biomass during early colonization.

192

193 *In vitro* growth assays confirm active metabolism by *S. alvi*

194 We next tested whether the putative host synthesized substrates were sufficient for growth of *S. alvi* as
195 sole carbon sources in a chemically defined liquid medium "Bee9", which we derived from standard
196 M9 media (**Fig. 4A**, **Dataset S3**). We utilized Bee9, after finding that *S. alvi* consumes amino acids
197 present in standard M9 previously used to grow this bacterium [12]. Only three metabolites (citrate,
198 isocitrate, and malate) supported growth as sole carbon sources in this condition. However, the addition
199 of 3Hmg, fumarate, succinate, gamma-aminobutyrate (Gaba), kynurenine, or urea to Bee9 + citrate
200 significantly improved the maximal growth rate of *S. alvi* relative to Bee9 + citrate alone (**Fig. 4B**). In
201 particular, 3Hmg and Gaba had dramatic effects on growth rates, increasing them 3.52 ± 0.10 and 2.76
202 ± 0.04-fold, respectively.

203 Analysis of the spent media revealed that all tested metabolites, except for the glucose negative control,
204 were depleted by *S. alvi* (**Fig. S6**). This further confirmed that the identified host-derived organic acids
205 are growth substrates of *S. alvi.* Unlike the results from our colonization experiments, *S. alvi* produced
206 numerous carboxylic acids, which varied based on the carbon source. For example, acetate was a
207 metabolic substrate, but it was also produced in the presence of pyruvate or 3Hmg. Meanwhile, alpha-
208 ketoglutarate, 2-oxoisovalerate, malate and succinate were produced across most growth conditions
209 (**Fig. 4C**). Consistent with the *in vivo* metabolomics, we detected production of anthranilate when
210 kynurenine was added to the media. Additionally, we also measured the production of kynurenic acid
211 and tryptophan (**Fig. 4D).** *S. alvi* wkB2 encodes a putative kynureninase gene in its genome
212 (SALWKB2_0716, Genbank genome: CP007446 [10]) that is likely responsible for the conversion of
213 kynurenine into anthranilate. Interestingly, this gene seems to have been acquired by horizontal gene
214 transfer as indicated by a phylogenetic analysis **(Fig. S7)**: apart from other *Snodgrassella* strains, the

closest sequences of the kynureninase gene were not found in other Neisseriaceae, but in more distantly related Betaproteobacteria (genera *Pusilimonas* and *Alcaligenes*) and in Gammaproteobacteria (genera *Ignatzschineria* and *Acinetobacter*).

Colonization without an exogenous nutrient source is conserved across strains of the genus *Snodgrassella*

As a final step, we examined whether our results were unique to *S. alvi* wkB2 type strain, or were more generally applicable to the genus, by inoculating bees with five divergent strains of *Snodgrassella*, three native to honey bees and two native to bumble bees. We also lengthened the colonization experiment from five to ten days to account for a potential delay in colonization of the honey bee gut by non-native strains. All five strains successfully colonized bees fed only sugar water. However, the efficiency and extent of colonization varied between strains. Strains of *Snodgrassella* native to honey bees colonized consistently, while non-native strains sometimes failed to colonize (Aggregate Colonization Success: 100% vs. 70%; Fisher's Exact test: $p < 0.001$) (**Fig. 5A**). The gut metabolomic comparison between successfully colonized versus MF bees was qualitatively similar to our initial results. Carboxylic acids, such as 3Hmg, malate, fumarate, succinate, isocitrate, and glycerate were significantly less abundant in colonized guts vs MF controls across three or more of the *S. alvi* strains tested. The levels of purine and amino acid precursors hypoxanthine and urea were also depleted in the guts of colonized bees, while anthranilate again accumulated in all colonized bees (**Fig. 5B, Fig. S8**). These results show that the utilization of host-derived carboxylic acids is a conserved phenomenon in the genus *Snodgrassella* and facilitates gut colonization independent of bacterial cross-feeding or diet-derived nutrients.

236

237 # Discussion

238 Host-derived metabolites are gaining appreciation for their importance in facilitating extracellular
239 microbial colonization across widely disparate animal models. In some cases, bacteria graze on the
240 chitinous lining of the murine gut or of light organ in squid [13-20]. In other instances, bacteria profit from
241 small molecules secreted into the lumen. Commensal species can utilize lactate, 3-hydroxybutyrate and
242 urea in the murine gut, while pathogenic *Salmonella* species utilize aspartate, malate, lactate or
243 succinate to invade the gut [21-24]. Our study demonstrates that this phenomenon is conserved across
244 widely disparate animal hosts and that these host-derived metabolites can represent the major carbon
245 source for certain gut bacteria facilitating colonization and growth, independent of the diet or cross-
246 feeding.

247 We took advantage of the bee as a model host to drastically minimize confounding factors, colonizing
248 bees with a single bacterium, *S. alvi,* while restricting the host to a sole dietary substrate that is
249 undigestible for this bacterium. We then utilized ^{13}C-glucose labelling to show that organic acids
250 measured in the gut are synthesized by the host from dietary sugars which are then assimilated by *S.*
251 *alvi* cells during gut colonization. The ^{13}C enrichment of *S. alvi* was initially higher than in the
252 surrounding host tissue, but then dropped after the host diet was switched to ^{12}C-glucose. These
253 dynamics are consistent with the hypothesis that *S. alvi* utilizes host metabolites that are derived from
254 simple carbohydrate catabolism in the bee diet, rather than from grazing on components of the host
255 epithelium lining in the gut (**Fig. 6**). Finally, we demonstrated that these organic acids sustain growth
256 of *S. alvi in vitro*.

257 Our results provide new context to the substantial body of research on bacterial colonization of the bee
258 gut. The consistent depletion of host-derived acids linked to the TCA cycle complements findings that
259 these metabolites are depleted in bees colonized with individual microbes including *S. alvi*, *Gilliamella,*
260 *Lactobacillus* Firm-5 and *Bartonella apis*, as well as when colonized with a full microbial community

261 [12,25,26]. Thus, foraging on host-derived compounds, although not always essential, may be widespread
262 in the native bee gut community. Yet, in the specific case of *S. alvi*, these host-derived nutrients seem
263 to be key for colonization. This is supported by a previous study which found that all genes of the TCA
264 cycle and multiple genes associated with organic acid and ketone body degradation, provide a strong
265 fitness advantage to *S. alvi* to grow in the bee gut [27].

266 Strikingly, two major metabolic functions conserved across all five strains of *S. alvi* (3Hmg
267 consumption and anthranilate production), were associated with unique features in the metabolic
268 pathways of *S. alvi*, providing evidence for adaptation to a specialized host niche. *S. alvi* possesses a
269 non-canonical TCA cycle (**Fig. 6**); lacking a glyoxylate shunt it is unable to grow on acetate alone, but
270 the substitution of acetate:succinate CoA-transferase for the canonical succinyl-CoA synthetase means
271 that acetate, rather than acetyl-CoA, is a key driver of the TCA cycle [28]. Interestingly, we found that
272 3Hmg consumption results in the production of acetate when *S. alvi* is grown on 3Hmg *in vitro*.
273 Therefore, we postulate that host-derived 3Hmg enhances growth of *S. alvi* via the production of acetate,
274 which in turn, increases the flux through the TCA cycle (**Fig. 6**). 3Hmg is an intermediate of the host's
275 isoprenoid biosynthesis, leucine degradation and ketone body metabolism, but the reason why this
276 metabolite is released into the gut remains elusive.

277 The second unique metabolic feature of *S. alvi*, the production of anthranilate, likely depends on the
278 enzymatic activity of a kynureninase gene identified in the genome of *S. alvi* converting host-derived
279 kynurenine into anthranilate (**Fig. 6**). Intriguingly, this is the only gene annotated in the tryptophan
280 degradation pathway of *S. alvi*; it is highly conserved in the entire genus and has likely been acquired
281 by horizontal gene transfer, suggesting that it encodes a conserved function that is specific to the
282 symbiosis between *Snodgrassella* and its bee hosts.

283 The release of relatively valuable metabolites into the gut could be a way for the host to control
284 community assembly and facilitate the colonization of particularly beneficial gut symbionts [29]. While
285 the full gut microbiota has been shown to carry out several important functions for the host, the specific
286 role of *S. alvi* has remained elusive. It is possible that its metabolic activities, such as the conversion of
287 kynurenine into anthranilate, has a positive effect on the host, such as protection against pathogen

288 invasion [30,31]. Kynurenine is important during the larval stage of bee development, but it is also
289 associated with neuronal defects (*e.g.*, hyperactivity and motor disfunction) in insects and vertebrates
290 [32-34]. In contrast, anthranilate is an important precursor of the essential amino acid tryptophan and
291 several neurotransmitters such as serotonin, tryptamine and various indole derivatives, all of which are
292 highly beneficial to bees [35]. Intriguingly, indoles synthesized from tryptophan by *Lactobacillus* Firm-5
293 species in the gut were recently linked to enhanced memory and learning in honey bees [36]. Finally, we
294 also note that the metabolism of urea by *S. alvi* could have a beneficial effect on the host. Urea
295 constitutes a major waste product in mammals and insects. In turtle ants, ancient, specialized gut
296 bacteria are able to recycle large amounts of nitrogen from urea into both essential and non-essential
297 amino acids [37]. We found that urea is more abundant in the bee gut when exogenous nitrogen was absent
298 from the diet, indicative of higher metabolic turnover and waste, which *S. alvi* could alleviate through
299 urea fixation.

300 Our results and analysis fit within the context of several limitations. We examined a portion of the total
301 gut metabolome that is amenable to analysis with gas chromatography. Further compounds of interest
302 may be detected using complimentary analytical capabilities. While we have shown that host-derived
303 compounds can sustain growth of *S. alvi*, the tested conditions did not reflect the natural state of the bee
304 gut with a full microbial community and a metabolically rich diet that alters between bee bread, pollen,
305 honey and flower nectar. Therefore, we cannot exclude that dietary or microbially-derived metabolites
306 contribute to the growth of *S. alvi* in the native gut. In fact, we found *in vivo* evidence for cross-feeding
307 of lactate and pyruvate from *Gilliamella*, as well as for pollen as an indirect source of key organic acids
308 in the gut. However, these nutrient sources seem to play a minor role relative to the host, as the
309 colonization levels of *S. alvi* did not differ significantly when pollen and/or *Gilliamella* were present.
310 This is consistent with a previous study, which showed that the total abundance of *S. alvi*, in contrast to
311 most other community members, does not change between nurse and forager bees that have different
312 dietary preferences, nor does it change when pollen is removed from the diet of fully colonized bees
313 under laboratory conditions [38].

314 How host synthesized organic acids reach the gut lumen remains elusive (**Fig. 6**). While leakage from
315 host cells across the epithelial barrier is possible, transport via the malpighian tubules upstream of the
316 ileum seems more likely, as they excrete nitrogenous waste and other metabolites into the gut while
317 also regulating osmotic pressure in the hemolymph [39,40]. Future work may resolve this question through
318 careful dissection and metabolomic analysis of the malpighian tubules and the ileum, possibly with the
319 assistance of labeled compounds injected into the bee thorax.

320

321 Methods

322 Bacterial culturing

323 **Table S1** lists all strains used in this study. Strains were isolated by directly plating gut homogenates
324 on brain heart infusion agar (BHIA), or by first culturing them in Insectagro™ (Gibco) liquid media
325 under microaerophilic conditions for 48 hours before colonies were streaked on plates. Species identity
326 was confirmed by 16S rRNA gene sequencing. Strains were grown on liquid Insectagro™ media for 18
327 hours and then diluted in Phosphate buffer saline (PBS) and 25% glycerol at OD_{600} =1. Solutions were
328 kept frozen at -80 °C until just before colonization, when they were thawed on ice, diluted 10-fold with
329 PBS and mixed 1:1 with sterile sugar water (1kg/L of sucrose in water).

330

331 Experimental colonization of gnotobiotic bees

332 All honey bees were collected from hives at the apiary of the University of Lausanne. A different hive
333 was selected for each colonization replicate. Microbiota-free bees were raised according to established
334 protocols [41]. Briefly, frames containing capped brood were taken from the hive and washed quickly
335 with a towel soaked in 3% bleach. Pupae of the appropriate age were then removed from the frames
336 and placed into sterile emergence boxes containing 0.2 µm filter sterilized sucrose (50% w/w) sugar
337 water. The boxes were placed in an incubator at 35 °C for 2 days, until the adult bees emerged. They

338 were then randomly transferred to separate, sterile cages assembled from plastic drinking cups and Petri
339 dishes.

340 Bees were colonized by hand with 5 µL of bacterial solution, or corresponding blank control, after
341 starving them of sugar water for 1-2 hours, stunning them on ice for 5 minutes, and transferring them
342 with tweezers to individual microcentrifuge tubes that were cut to enable insertion of a pipette tip. Sugar
343 water and, where specified, polyfloral pollen (Bircher Blütenprodukte) sterilized via electron beam
344 irradiation (Studer Cables AG) were provided to cages *ad libitum* throughout each experiment. Mono-
345 and co-colonization of bees with *S. alvi* wkB2 and the four *Gilliamella* strains were performed five
346 times, using different hives for each treatment. Not all conditions were run in each experiment due to
347 technical difficulties preparing the treatment groups, and the GC-MS analysis was only carried out for
348 a subset of the samples (see **Table S2** for details**)**. The colonization experiment with the divergent
349 *Snodgrassella* strains isolated from honey bees and bumble bees was carried out twice (see **Table S3**
350 for details).

351 At the end of each experiment, bees were anesthetized with CO_2, placed on ice, and dissected with
352 sterile forceps. Whole guts, minus the crop, were homogenized in a bead beater (FastPrep-24, MP) in
353 tubes containing PBS and glass beads. The samples were each immediately divided into three aliquots.
354 One was plated to count Colony Forming Units (CFUs) on BHIA as well as for contaminants on
355 Nutrient agar (NA) and De Man, Rogosa and Sharpe agar (MRSA). Another aliquot of 500 µL was
356 centrifuged for 15 minutes at 4 °C and 20,000 g^{-1} and the liquid supernatant snap frozen in liquid
357 nitrogen and stored at -80 °C until metabolomic extraction. The third aliquot was frozen at -80 °C until
358 DNA extraction.

359

360 ## Validation of bee sterility

361 To rule out contamination in the guts of newly emerged bees, two bees from each emergence box in
362 each experiment were sacrificed and 10 µL of their homogenized guts plated on BHIA (5% CO_2), NA
363 (aerobic) and MRSA (anaerobic) at 35ºC to check for sterility prior to colonizing the remaining bees.

364 In the event of contamination detected in newly emerged bees, all bees from that emergence box were
365 discarded from the experiment. The same contamination checks were also performed on all analyzed
366 bees at the end of each experiment. Additional sterility checks were performed in the experiment where
367 we compared gut metabolite levels in newly emerged and six-day old MF bees. Here we also plated
368 eight homogenized guts on Potato dextrose agar (PDA, aerobic), Lysogeny broth agar (LBA, aerobic),
369 Tryptic soy agar (TSA, 5% CO_2), Columbia agar + 5% sheep blood (CBA+5%SB, 5% CO_2 &
370 anaerobic), and Tryptone yeast extract glucose agar (TYG, anaerobic).

371

372 Quantification of pollen consumption

373 Both whole bees and dissected bee guts were weighed to assess treatment effects and quantify pollen
374 consumption. Whole bee and wet gut weights were both significantly higher in bees provided pollen
375 than in those provided sugar water only, while colonization did not significantly affect weight (**Fig. S4**).
376 (Linear mixed effects models fitted by ML with nested, random cage effects: [Bee weight, n=271, Diet:
377 $F_{(1,262)}$=176.1, p<.001; *S. alvi*: $F_{(1,262)}$=0.1, p=.769; *Gilliamella*: $F_{(1,262)}$=1.0, p=.311; *S. alvi:Gilliamella*:
378 $F_{(1,262)}$=0.7, p=.388]; [Gut weight, n=271, Diet: $F_{(1,262)}$=220.0, p<.001; *S. alvi*: $F_{(1,262)}$=0.3, p=.595;
379 *Gilliamella*: $F_{(1,262)}$=0.02, p=.880; *S. alvi:Gilliamella*: $F_{(1,262)}$=2.3, p=.131]. We also weighed filled
380 pollen troughs at the beginning and end of the experiment and calculated the amount of pollen consumed
381 per bee. Unsurprisingly, the mean difference in gut weights between dietary groups (22.3 ± 18.3 mg/bee)
382 closely matched the measured amount of pollen consumed by the bees across colonization treatments
383 (24.3 ± 7.2 mg/bee) (**Table S2**). We then calculated the bee body weight (bee weight – gut weight) to
384 determine if diet or colonization led to actual tissue weight gain in bees. While we found a slight
385 increase in body weight from pollen (95% CI [0.69 mg, 7.51 mg]), we cannot rule out that this was in
386 fact due to variable amounts of pollen present in the crop, which was not removed with the hindgut (Gut
387 weight, n=271, Diet: $F_{(1,262)}$=5.2, p=.023; *S. alvi*: $F_{(1,262)}$=1.4, p=.240; *Gilliamella*: $F_{(1,262)}$=0.6, p=.442;
388 *S. alvi:Gilliamella*: $F_{(1,262)}$=3.8, p=.052).

389

390 ## Isotope tracing experiments

391 To assess the ^{13}C metabolite enrichment in the bee gut, MF bees were provided a 45:65 ratio of 99%
392 uniformly labelled U-$^{13}C_6$ glucose (Cambridge Isotope Laboratory) and naturally abundant sucrose
393 (Sigma Aldrich) in the first experiment. For the NanoSIMS time-course colonization experiment, newly
394 emerged MF bees were divided into two cages and provided pure 99% U-$^{13}C_6$ glucose (treatment) or
395 naturally abundant (*i.e.* ~98.9% ^{12}C) -glucose (control) in water for five days (pulse) before switching
396 both cages to a naturally abundant glucose diet (chase). On the morning of the fourth day all bees were
397 starved for 1.5 hours and colonized with *S. alvi* wkB2. The ^{13}C glucose solution was replaced with a
398 ^{12}C glucose solution 24 hours later. Bees were harvested at 0, 8, 24, 32, 48, 56, 72 hours after
399 inoculation. This overlap of colonization and ^{13}C glucose feeding was chosen to both maximize the
400 number of bacterial cells in the TEM sections and to reduce the dilution of ^{13}C label due to metabolic
401 turnover. For each timepoint and both cages (^{13}C and ^{12}C glucose treatment), the ileum of four bees
402 were dissected. One gut was immediately preserved for electron microscopy and NanoSIMS, while the
403 other three guts were homogenized and aliquoted for CFU plating and metabolite extraction **(Fig. 3)**.
404 The control samples (from the cage provided with ^{12}C glucose) were used to determine the natural ^{13}C
405 abundance in the bee tissue and *S. alvi* cells. Image metadata and Raw NanoSIMS region of interest
406 (ROI) values can be found on github: https://github.com/Yelchazli/Foraging-on-host-synthesized-
407 metabolites-enables-S.-alvi-to-colonize-the-honey-bee-gut.

408

409 ## Quantification of bacterial loads via qPCR

410 DNA extraction was carried out by adding 250 µL of 2x CTAB to frozen gut homogenates. The mixture
411 was homogenized at 6 m/second for 45 seconds in a Fast-Prep24TM5G homogenizer (MP Biomedicals)
412 and centrifuged for 2 minutes at 2000 rpm. DNA was extracted in two-steps with Roti-Phenol and
413 Phenol:Chloroform:Isoamylalcohol (25:24:1), then eluted in 200 µL DNAse/RNAse water and frozen.
414 qPCR was run using target-specific primers for *Apis mellifera* actin, and specific 16S rRNA gene
415 primers for *S. alvi* and *Gilliamella spp.* as well as 16S rRNA gene universal primers used in [12]. qPCR

416 reactions were run on a QuantStudio 3 (Applied Biosystems), and standard curves were performed using
417 the respective amplicons on a plasmid as previously described [12].

418 In addition, 18S rRNA gene amplification with universal primers were run to assess fungal loads (F:
419 TATGCCGACTAGGGATCGGG, R: CTGGACCTGGTGAGTTTCCC) [42]. qPCR reactions were run
420 on 384-well plate QuantStudio 5 (Applied Biosystems). The corresponding standard curve for absolute
421 quantification was performed using the 199 bp amplicon as opposed to a plasmid containing the
422 amplicon. Data was extracted and analyzed as previously described [12].

423

424 Metabolite extractions

425 Frozen gut samples were divided and extracted via two established methods for short chain fatty acids
426 (SCFAs) and soluble metabolites. Prior to soluble metabolite extraction from pure pollen grains, an
427 equivalent amount to what was digested per bee was mixed with PBS. In order to approximate physio-
428 chemical degradation of the pollen in the bee gut, the samples were bead beaten and incubated at 35ºC
429 for 18 hours.

430 SCFAs were extracted with 750 µL diethyl ether from 75 µL of gut supernatant that was first acidified
431 with 5 µL of 11% HCl. Isovalerate [200 µM] (Sigma Aldrich) was used as an internal standard. The
432 solvents and resulting two-phase mixture were kept cold at -20 °C and vortexed 3x for 30 seconds. The
433 samples were then centrifuged for 3 minutes at 4 °C and 13000 g^{-1}, and 80 µL of the ether phase was
434 removed to a glass GC vial (Agilent). The sample was derivatized with 20 µL MTBSTFA + 1% TBDMS
435 (Sigma Aldrich) for 1 hour at 30 °C [43].

436 Soluble metabolites were extracted via a modified Bligh and Dyer protocol [44]. A (5:2:1) mixture of
437 methanol (Sigma Aldrich) and chloroform (Sigma Aldrich) and double distilled water was chilled to -
438 20 °C and 800 µL added to 100 µL of gut homogenate. A mixture of norleucine (Sigma Aldrich),
439 norvaline (Sigma Aldrich), and ^{13}C glucose (Cambridge Isotopes) was used as internal standards. The
440 samples were vortexed three times for 30 seconds and extracted at -20 °C for 90 minutes. The samples
441 were then centrifuged at 13,300 g^{-1} and 4 °C for 5 minutes. Liquid supernatant was transferred to a new

442 tube and 400 µL of cold chloroform : methanol (1:1) was added to the insoluble material. The samples
443 were again vortexed three times, extracted for 30 minutes at -20 °C, centrifuged, and the two
444 supernatants were combined. Phase separation was achieved by adding 200 µL of water and
445 centrifuging at the same conditions. The upper phase was then dried overnight in a speed vacuum. The
446 sample was derivatized with 50 µL of 20 mg/mL methoxyamine hydrochloride in pyridine (Sigma
447 Aldrich), for 90 minutes at 33 °C followed by silylation with 50 µL of MSTFA (Sigma Aldrich) for 120
448 minutes at 45 °C.

449

450 ## GC-MS analysis

451 Samples were analyzed on an Agilent 8890/5977B series GC-MSD equipped with an autosampler that
452 injected 1 µL of sample onto a VF-5MS (30m x 0.25 mm x 0.25 um) column. The SCFA samples were
453 injected with a split ratio of 25:1, helium flow rate of 1 mL/min, and inlet temperature of 230 °C. The
454 oven was held for 2 minutes at 50 °C, raised at 25 °C/min to 175 °C and then raised at 30 °C/minute to
455 280 °C and held for 3.5 minutes. The MSD was run in SIM mode with 3 target ions for each compound.
456 The Soluble metabolite samples were injected with a split ratio of 15:1, helium flow rate of 1 mL/min
457 and inlet temperature of 280 °C. The oven was held for 2 minutes at 125 °C, raised at 3 °C/minute to
458 150 °C, 5 °C/minute to 225 °C, and 15 °C/minute to 300 °C and held for 1.3 minutes. The MSD was
459 run in scan mode from 50-500 Da at a frequency of 3.2 scan/second.

460

461 ## Metabolomics data analysis

462 Mass spectrometry features were identified by spectral matching to the NIST17 mass spectra library or
463 to in house analytical standards. Features were then extracted using the MassHunter Quantitative
464 Analysis software (Agilent). Data normalization and analysis was performed using custom R scripts
465 (See Data availability). Absolute metabolite quantification was performed by fitting normalized
466 response values to calibration curves of analytical standards. The effect of diet, and colonization with
467 *S. alvi* and *Gilliamella* were assessed by fitting z-score normalized metabolite abundances to a mixed

468 linear model using the lmm2met package in R with diet, *S. alvi* and *Gilliamella* as fixed effect factors
469 and experimental replicate as a random effect [45]. The significance of each fixed effect was then adjusted
470 by the Benjamini, Hochberg, and Yekutieli method to control for false discovery. Mass isotopologues
471 were adjusted to account for natural isotope abundances following published procedures [46,47].

472

473 ## TEM section preparation and NanoSIMS analysis

474 Bee guts were dissected, the ileum was cut away from the rest of the gut and fixed in glutaraldehyde
475 solution (EMS, Hatfield, PA, US) 2.5% in Phosphate Buffer (PB 0.1M pH7.4) (Sigma, St Louis, MO,
476 US) for 2 hours at room temperature (RT) and kept at 4°C until sample preparation. Ileum pieces were
477 rinsed 3 times for 5 minutes in PB buffer and then postfixed with a fresh mixture of osmium tetroxide
478 1% (EMS, Hatfield, PA, US) with 1.5% potassium ferrocyanide (Sigma, St Louis, MO, US) in PB
479 buffer for 2 hours at RT. The samples were then washed three times in distilled water and dehydrated
480 in acetone solution (Sigma, St Louis, MO, US) at graded concentrations (30%-40min; 70%-40min;
481 100%-1h; 100%-2h). Dehydration was followed by infiltration in Epon resin (Sigma, St Louis, MO,
482 US) at graded concentrations (Epon 1/3 acetone-2 hours; Epon 3/1 acetone-2 hours, Epon 1/1-4 hours;
483 Epon 1/1-12 hours) and finally polymerized for 48 hours at 60°C in an oven. Thin sections of 100
484 nanometers (nm) were cut on a Leica Ultracut (Leica Mikrosysteme GmbH, Vienna, Austria) and
485 picked up on copper slot grid 2x1mm (EMS, Hatfield, PA, US) coated with a Polyetherimide (PEI) film
486 (Sigma, St Louis, MO, US). Sections were poststained with uranyl acetate (Sigma, St Louis, MO, US)
487 2% in H_2O for 10 minutes, rinsed several times with H_2O followed by Reynolds lead citrate for 10
488 minutes and rinsed several times with H_2O.

489 Large montages with a pixel size of 6.9 nm covering areas of around 120x120 µm were taken with a
490 transmission electron microscope Philips CM100 (Thermo Fisher Scientific, Hillsboro, USA) at an
491 acceleration voltage of 80kV with a TVIPS TemCam-F416 digital camera (TVIPS GmbH, Gauting,
492 Germany) and the alignment was performed using Blendmont command-line program from the IMOD
493 software [48].

494 Four holes were made using the electron beam at the four corners of the montage to localize the area of
495 interest for NanoSIMS imaging. Then the slot grid was deposited on 1 µL of distilled water on a 10 mm
496 round coverslip and left to dry for 10 minutes. The slot grid was detached, letting the section attach to
497 the coverslip.

498 After being coated with a 15nm gold layer to evacuate a potential build-up of a charge during the
499 NanoSIMS analyses, the samples were analyzed by a NanoSIMS 50L (CAMECA). A primary beam of
500 16 keV Cs+ ions was focused to a spot size of about 100 nm on the sample surface, causing the
501 sputtering of atoms and small molecules from the first 5-10 nm of the sample. Negative secondary ions
502 were directed and focalized into a single beam before reaching the magnetic sector of the mass
503 spectrometer where the ions were separated. The species of interest ($^{12}C^{14}N$- and $^{13}C^{14}N$- for this study)
504 were then measured simultaneously using Electron Multipliers. To resolve the interference between
505 $^{13}C^{14}N$- and $^{12}C^{15}N$-, two slits (ES and AS) were used to achieve a mass resolution higher than 10000
506 (Cameca definition), [49].

507 In the imaging mode, selected areas of 25x25 µm were implanted using a strong beam (using diaphragm
508 D1-1 (diameter 750 µm) and a current of 16 pA) to remove the gold coating and reach stable emission
509 conditions. After optimization of the extraction of the secondary ions, the area was imaged by scanning
510 with a smaller beam (~100 nm, using diaphragm D1-5 (diameter 100 µm) and a current of 0.45 pA)
511 with a 256x256 pixel resolution and a dwell time of 5µs/pixel. For each image, 10 layers were acquired.
512 The image processing was performed using "L'image" software (Larry Nittler, Carnegie Institution of
513 Washington). The 10 layers were aligned and stacked, 44 ms deadtime correction was applied. Regions
514 of interests (ROI) were manually drawn around bacterial cells, gut epithelium layer, and bulk host cells.
515 The resulting data is reported in **Dataset S1**. At% enrichment was calculated in R using the data.table
516 package. At% enrichment formula: $13C\ At\% = {}^{14\mathrm{N}\ 13\mathrm{C}}/_{(14\mathrm{N}\ 13\mathrm{C}\ +\ 14\mathrm{N}\ 12\mathrm{C})} \times 100$. **(Fig. S9).**

517

518 ## *In vitro* growth of *S. alvi*

519 *S. alvi* was cultured in Bee9 media, an M9-derived minimal defined media containing essential vitamins
520 and mixtures of organic acids (see recipe in **Dataset S3** on github:
521 https://github.com/Yelchazli/Foraging-on-host-synthesized-metabolites-enables-S.-alvi-to-colonize-
522 the-honey-bee-gut). Growth assays were performed in 96-well plates (Corning costar) at 35 °C, 5%
523 CO_2, with continuous orbital shaking (H1 Synergy, Biotek). OD_{600} measurements were taken every 30
524 minutes for 20 hours. All conditions were independently replicated three times. For metabolomics
525 measurements, plates were immediately placed on ice at the end of each experiment, and liquid was
526 transferred to microcentrifuge tubes. The tubes were then centrifuged at 13,300 g and 4 °C for 30
527 seconds, and the liquid supernatant was then snap frozen in liquid nitrogen and stored at -80 °C for
528 metabolomic analysis.

529

530 ## Phylogenetic analysis of the kynureninase gene family

531 The kynureninase protein sequence of *S. alvi* wkB2 was retrieved from NCBI (WP 025330329.1), and
532 blasted (NCBI, BlastP) against the "nr" database. Based on the BlastP hits, 227 divergent amino acid
533 sequences were exported in fasta format and aligned using MUSCLE [50] with standard parameters. Tree
534 inference and bootstrap validation were performed using IQtree with the following command: "iqtree-
535 omp -s kyn_sequences_muscle.aln -nt 6 -m TEST -bb 1000" [51]. The tree topology was visualized using
536 the ITOL online viewer (https://itol.embl.de/).

537

Data Availability

Raw data and scripts used to process data and generate figures are available on github at the following link: https://github.com/Yelchazli/Foraging-on-host-synthesized-metabolites-enables-S.-alvi-to-colonize-the-honey-bee-gut. Metabolomics data have been deposited to the EMBL-EBI MetaboLights database (DOI: 10.1093/nar/gkz1019, PMID:31691833) with the identifier MTBLS8058. https://www.ebi.ac.uk/metabolights/MTBLS8058

Acknowledgments

We would like to thank Silvia Moriano-Gutierrez, and Gonçalo Santos-Matos for providing helpful comments on the manuscript. This work was funded by the University of Lausanne, an ERC Starting Grant (MicroBeeOme), the NCCR Microbiomes, a National Centre of Competence in Research, funded by the Swiss National Science Foundation (grant no. 180575) and a Swiss National Science Foundation project grant (grant no. 179487) to P.E.

Author Contributions

A.Q., Y.E. and P.E. conceived the project and designed the experiments. A.Q, and Y.E. performed the experiments. A.Q. analyzed the GC-MS results, while Y.E. analyzed the qPCR and NanoSIMS results. N.N. assisted with bee experiments, metabolite, and DNA extractions. A.M.N. performed preliminary in vitro growth experiments. J.D. performed the tissue sectioning and TEM imaging supervised by C.G. S.E. performed the NanoSIMS imaging and instructed on the data analysis, supervised by A.M., who also advised on the design of the NanoSIMS experiment. A.Q., Y.E. and P.E. wrote the manuscript, with contributions from S.E. and A.M. All authors reviewed the manuscript and provided feedback. As equally contributing first authors, A.Q. and Y.E. may each list their name first when referencing this work.

Figures

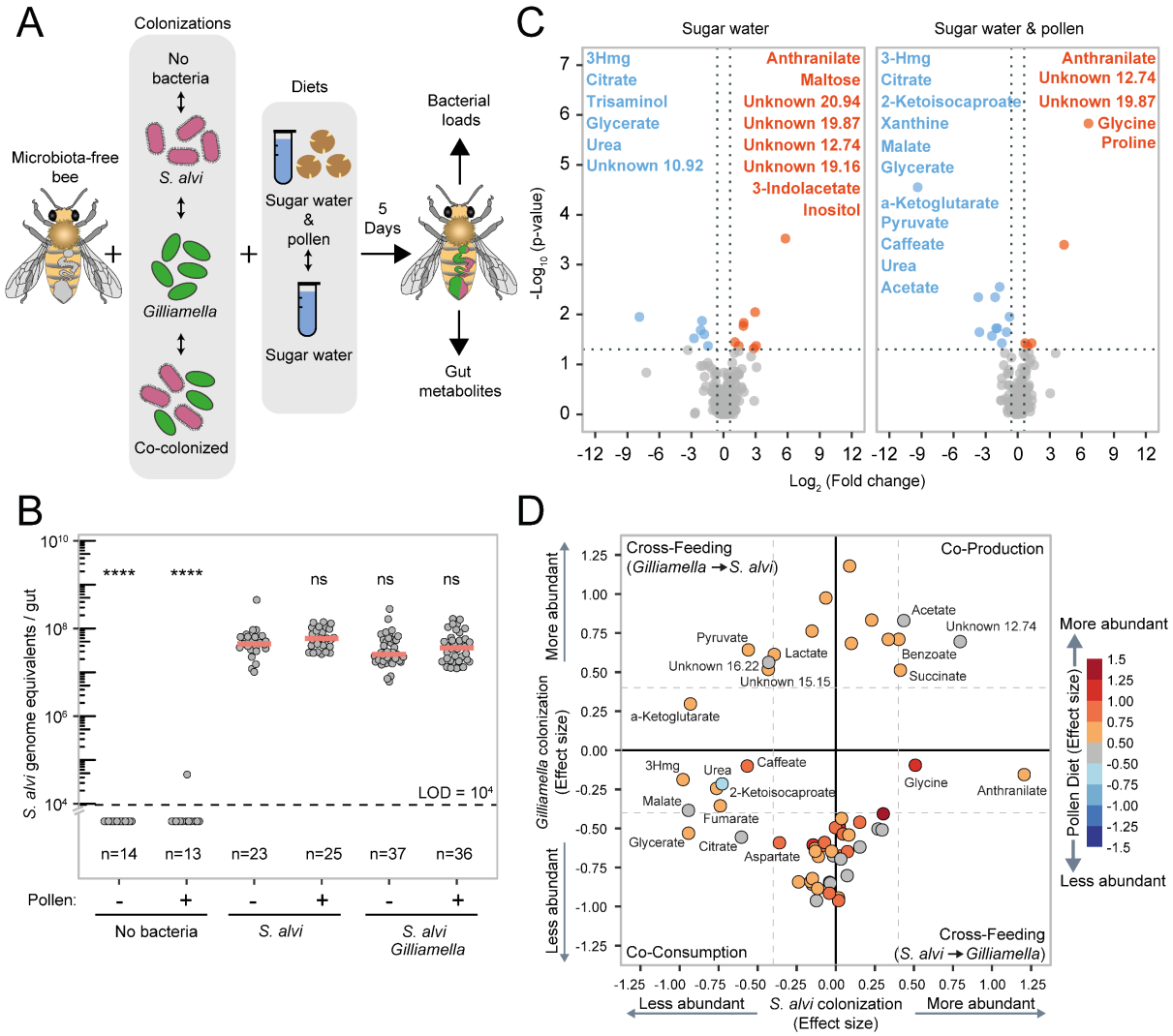

Figure 1. *S. alvi* colonizes bees fed with sugar water only and depletes host, pollen, and *Gilliamella*-derived metabolites. (A) Outline of the bee colonization experiment with four colonization treatments (no bacteria, *S. alvi*, *Gilliamella*, or co-colonized) and two dietary treatments (sterile sugar water and pollen, or sterile sugar water only). Five days after colonization gnotobiotic bees were sacrificed and the bacterial load and the metabolites in the gut quantified. **(B)** Number of *S. alvi* cells (number of bacterial genome equivalents) per bee gut determined by qPCR using *S. alvi*-specific 16S rRNA gene primers. Each value represents the number of cells in a single bee gut, red bars represent the median,

horizontal black line represents qPCR limit of detection (LOD = < 10^4). For each treatment, the presence/absence of pollen in the diet is indicated by +/- sign. Significance determined by Wilcoxon rank sum test with *S. alvi* (pollen -) as reference group, ns, non-significant; ****$P < 0.001$. **(C)** Significantly differentially abundant gut metabolites between *S. alvi* colonized and MF bees (i.e., 'no bacteria' treatment). Significantly depleted and produced metabolites are shown in blue and orange, respectively. Adjusted significance values were calculated using Wilcoxon rank sum test, and Benjamini-Hochberg correction, using the MF samples as a reference. **(D)** Results from mixed-linear modelling show the contributions (fixed effect sizes) of microbial colonization and diet towards z-score normalized metabolite abundances. Only metabolites significantly correlated with *S. alvi* colonization are named. Large values (+/-) indicate a strong correlation between a factor and a corresponding change in metabolite abundance. Values centered around zero (inside the dotted lines) are not significant. The effect size of pollen is indicated by the color of each metabolite, red colors indicate significantly positive correlation, while blue is a significant negative correlation. The four corners of the graph represent the four types of metabolic interactions between *S. alvi* and *Gilliamella* (from the top left: cross-feeding from *S. alvi* to *Gilliamella*, co-production by both bacteria, cross-feeding from *Gilliamella* to *S. alvi,* co-consumption). Carboxylic acids are grouped principally on the lower-left section of the plot indicating they are less abundant with *S. alvi* and *Gilliamella* colonization.

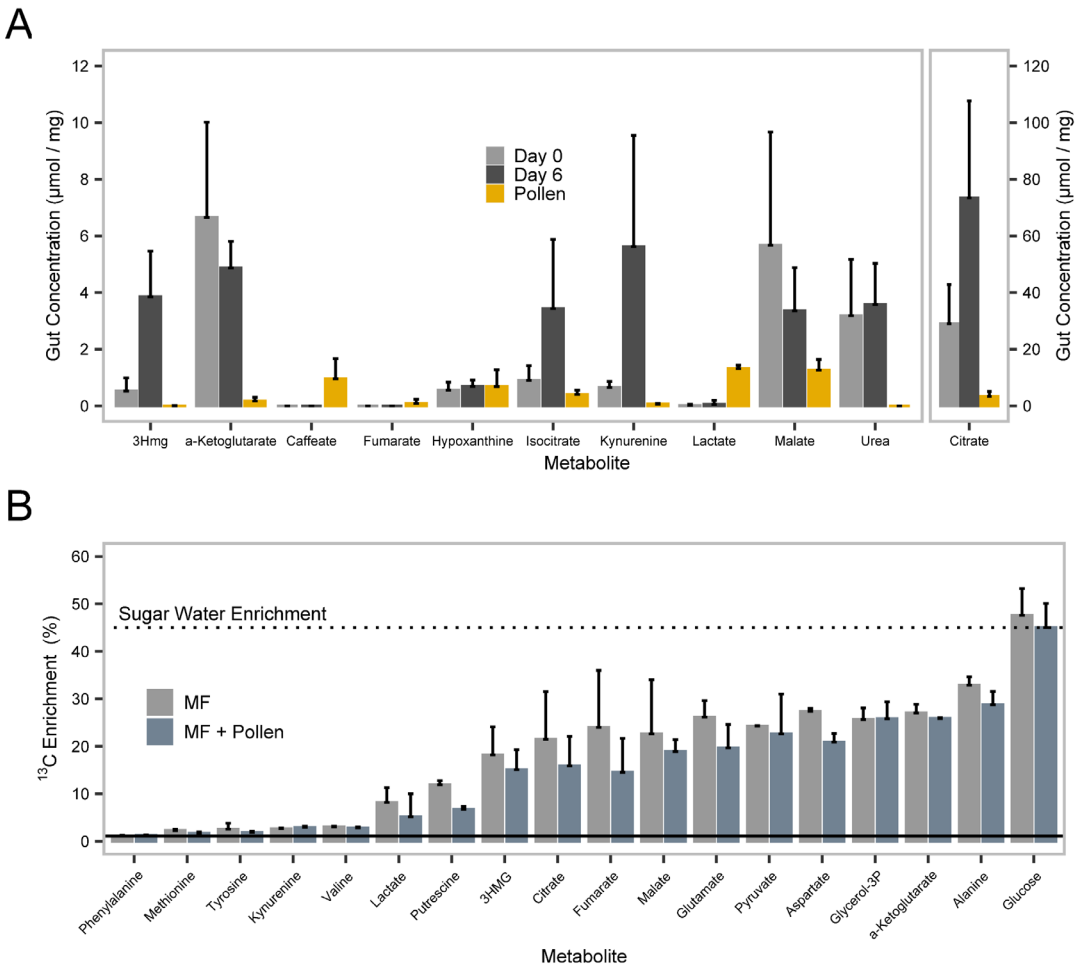

Figure 2. Gut metabolite abundances and isotope labelling reveals the host origin of *S. alvi* substrates. (A) Abundances of selected metabolites in the guts of MF bees increase from emergence (Day 0) to adult age (Day 6) (n=8). All metabolites except for caffeate and lactate were less abundant when extracted directly from an equivalent amount of pollen consumed per bee over six days (n=8). Quantitates from pollen extract were adjusted based on average total pollen consumption per bee (see methods). **(B)** The average (n=4) ^{13}C metabolite enrichment (%) in bee guts shows that carboxylic acids and non-essential amino acids become highly labelled upon feeding ^{13}C-glucose to MD bees. Dark and light bars indicate, respectively, absence and presence of pollen in the diet. The solid line denotes the natural ^{13}C enrichment (1.108%), while the dashed line denotes ^{13}C enrichment of sugar water solution fed to experimental bees.

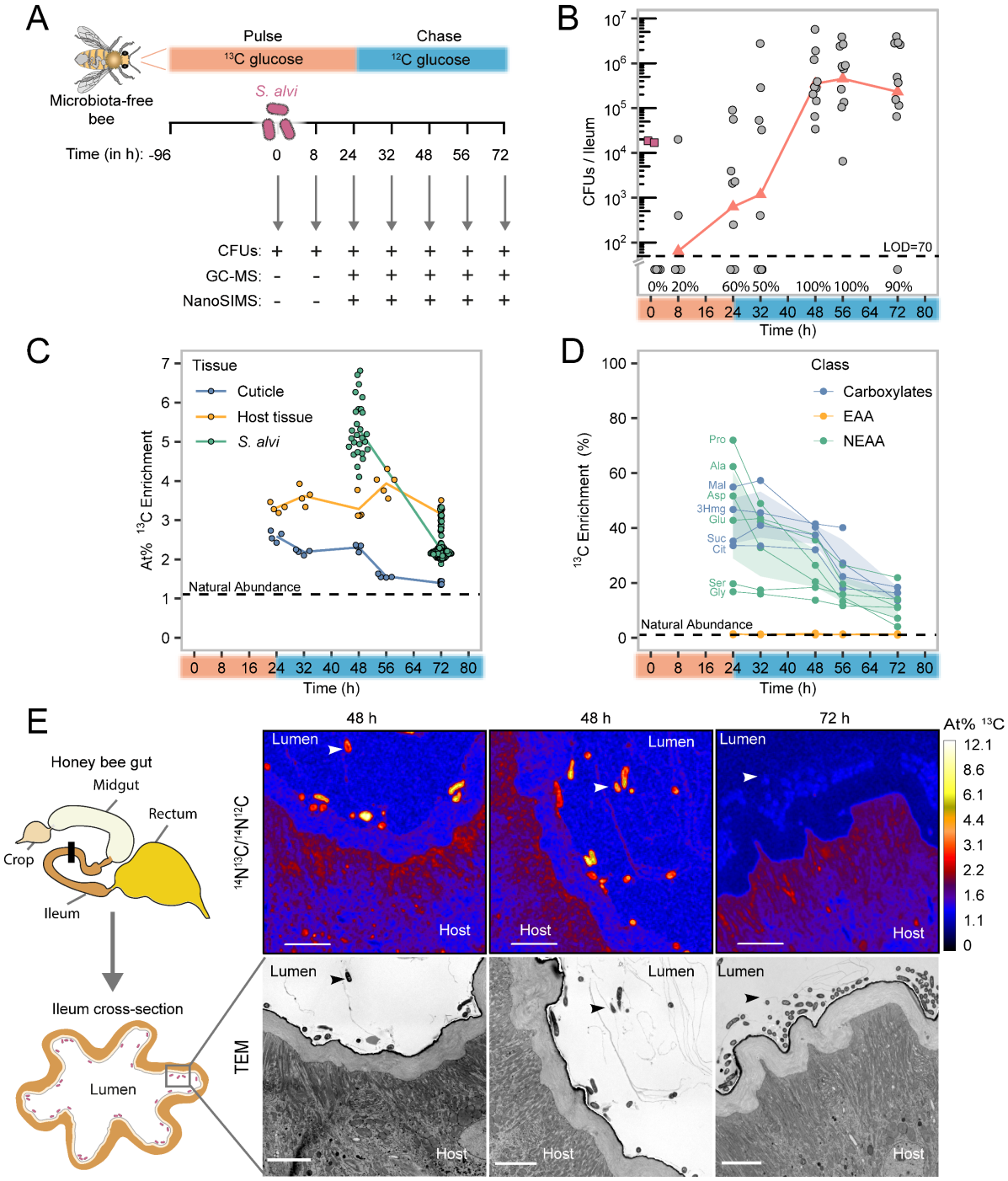

601

602 **Figure 3. *S. alvi* builds biomass from substrates derived from the glucose metabolism of the host.**

603 **(A)** Experimental design of the pulse-chase isotope labelling gnotobiotic bee experiment. Newly

604 emerged MF bees were fed 100% ^{13}C glucose for four days (i.e., 96 hours), colonized with a defined

605 quantity of *S. alvi* and then the ^{13}C glucose was replaced by ^{12}C glucose 24 hours after colonization. The

606 timeline indicates when bees were sampled for CFU plating, GC-MS and NanoSIMS analysis relative

607 to the timepoint of colonization (i.e. 0h). **(B)** Colonization levels of *S. alvi* in the ileum until 72 hours

post inoculation show the initial strong colonization bottleneck and subsequent exponential increase in cell numbers. Colonization success is indicated as percentage of bees with detectable CFUs. Pink squares indicate the inoculum of *S. alvi* (OD= 0.1). The limit of detection (LOD) of 70 CFUs per ileum is indicated with the dashed line. **(C)** The average At% ^{13}C enrichments of *S. alvi* cells decreases rapidly, while the enrichment of host cells and epithelium remains constant over 72 hours in ileum cross-sections imaged with NanoSIMS. Each data point represents the mean of regions of interest (ROI); bacterial ROIs consist of single bacterial cells, while epithelium and host cells ROIs represent the total area encompassing epithelium or host cell tissue in each image. ROI raw counts and calculated enrichments are listed in **Dataset S1**. The dashed line at 1.1 % indicates the natural ^{13}C abundance calculated from NanoSIMS images of ^{12}C control bees. **(D)** ^{13}C enrichment of metabolites in the gut steadily decreases in the ^{12}C chase phase. Values represent the average ^{13}C enrichment of a given metabolite across the bees sampled at that timepoint. Average values and colors are shown by metabolite class: carboxylic acids (violet), non-essential amino acids (NEAA, green), essential amino acids (EAA, brown). Measured metabolites are listed in **Dataset S1**. The dotted line at 1.1 % indicates the natural ^{13}C abundance. **(E)** NanoSIMS and corresponding TEM images of 2 different ^{13}C labeled bees at 48 and 72 hours after inoculation. White arrows indicate *S. alvi* cells. At% ^{13}C represents percentage of ^{13}C atoms; the natural ^{13}C abundance is ~1.1 at%. Scale bars = 5 μM. Schematic drawing of the honey bee gut shows the region in the ileum (black bar) where cross-sections were taken and which regions of the cross-sections were imaged.

628

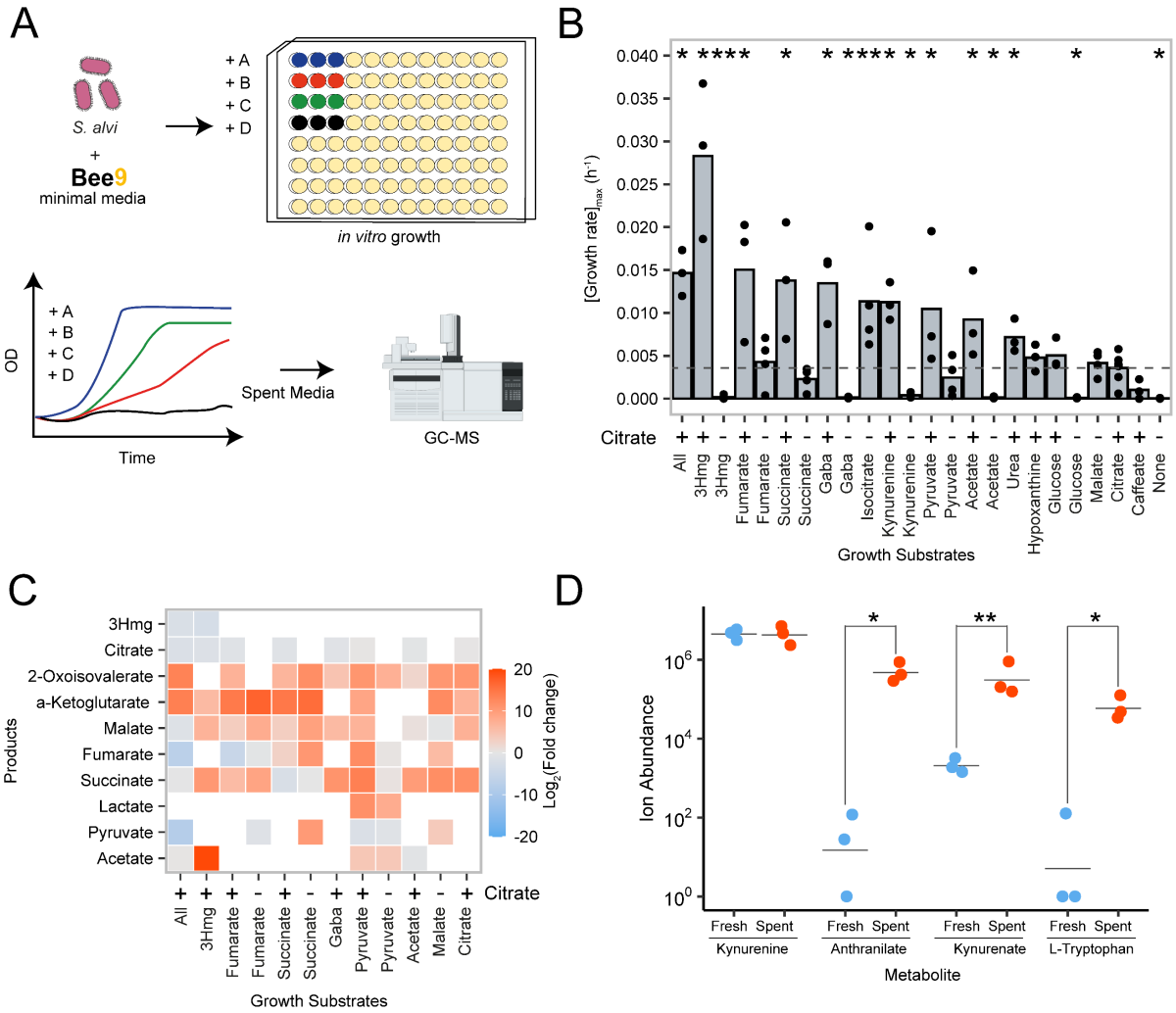

629

630 **Figure 4**. **Host synthesized compounds enhance *S. alvi* growth *in vitro*. (A)** Schematic diagram
631 depicting growth and spent supernatant analysis. The "Bee9" media was derived from M9 base media
632 (**Dataset S3**). **(B)** The maximum growth rate across single carbon sources with (+) or without (-) citrate
633 added to the medium, reveals that growth on citrate + 3Hmg was faster than for all other conditions,
634 including "All", where all substrates were pooled together. The average value (bars) was calculated
635 from the individual biological replicates (dots). Adjusted significance values were calculated using
636 Wilcoxon rank sum test, and Benjamini-Hochberg correction, using the growth on citrate as the
637 reference state (dotted line). **(C)** Abundances of carboxylic acids in the spent supernatant, relative to
638 growth on citrate alone, varies with growth substrates. While some carboxylic acids including a-
639 ketoglutarate and malate are produced across most conditions, acetate is a growth substrate, but only

640 produced with either pyruvate or 3Hmg in the media. **(D)** Addition of kynurenine to the media leads to
641 the production of anthranilate, kynurenic acid, and L-tryptophan. Significant changes between fresh and
642 spent media were calculated using a paired t-test. (* P < 0.05, ** < 0.01, *** < 0.001, **** < 0.0001).

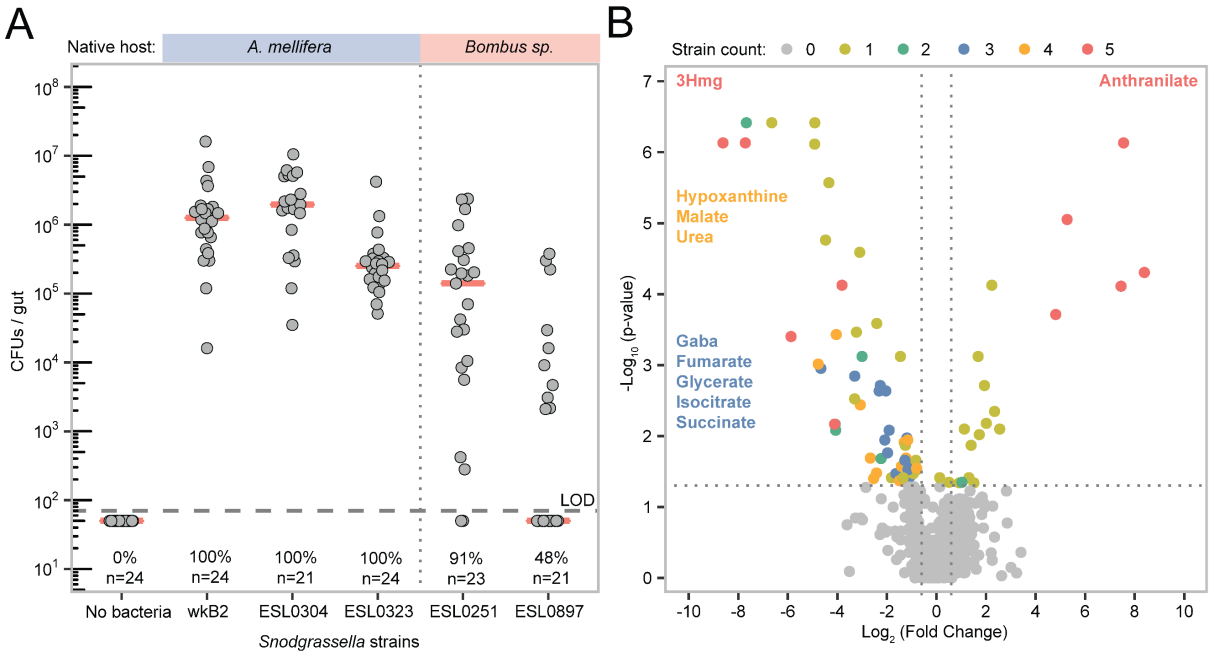

643

644 **Figure 5. Gut colonization in the presence of a sugar-restricted diet and depletion of host-derived**
645 **metabolites is conserved across divergent *Snodgrassella* strains. (A)** Colonization levels of
646 divergent *Snodgrassella* strains in monocolonized bees. Pink bars denote the median of CFUs/gut for
647 each group. The LOD=70 colonies/gut is shown with a horizontal dashed line. The top bar indicates
648 *Snodgrassella* strains native to *A. mellifera* versus *Bombus sp.* Colonization success (%) is shown for
649 each strain, defined as guts with detectable CFU counts. (**B**) Volcano plot of gut metabolites showing
650 the similarities in metabolite changes from MF vs colonized bees across strains. Each metabolite is
651 plotted five times (once per *Snodgrassella* strain), and color coded by the number of strains in which it
652 is significantly differentially abundant vs MF bees control. Only 3Hmg and anthranilate were
653 significantly depleted or enriched by all five strains, while four of the strains depleted hypoxanthine,
654 malate, and urea, and three of the five depleted Gaba, fumarate, glycerate, isocitrate and succinate.

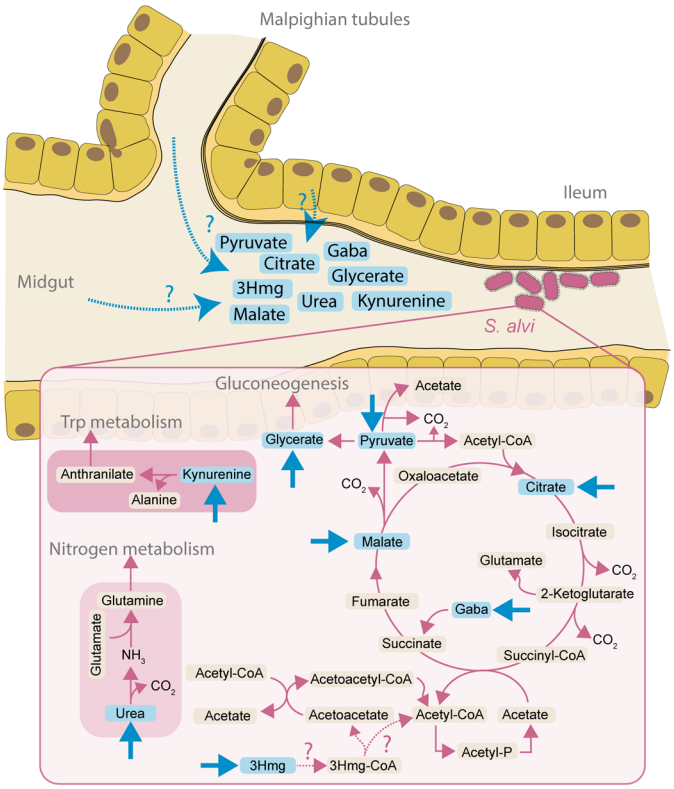

Figure 6. Schematic model of *S. alvi* metabolism of host-derived compounds in the ileum. Host metabolites (blue) enter the ileum through the epithelial cells, or through the malpighian tubules upstream of the ileum. *S. alvi* primarily utilizes the TCA cycle to generate energy, then synthesizing biomass through gluconeogenic reactions. 3Hmg provides a source of acetate to fuel the TCA cycle. However, the reactions synthesizing the first two steps (dotted pink arrows) have not been annotated in the genome. Additionally, host synthesized urea is a source of nitrogen, and kynurenine is converted to anthranilate as part of tryptophan metabolism. Blue arrows indicate the entry of substrates provided by the host metabolism.

Supplementary Figures and Tables

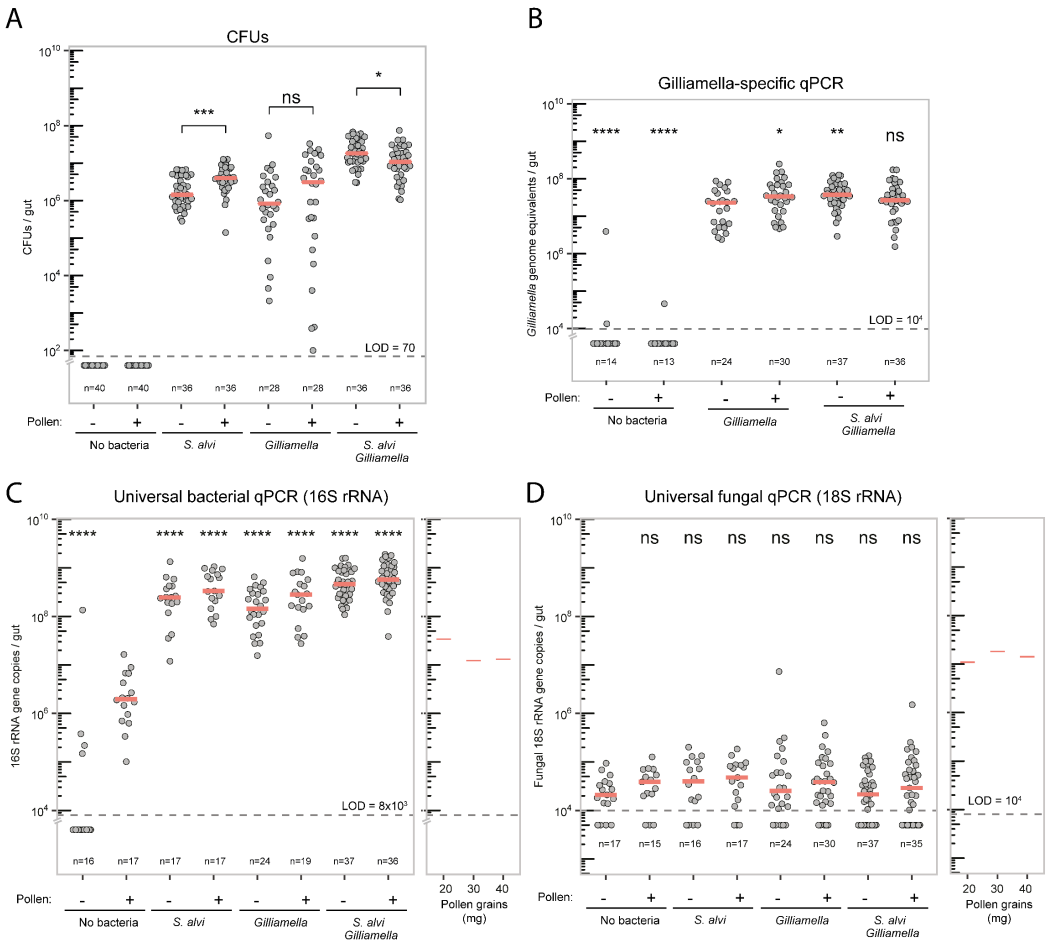

Figure S1. Total number of bacteria and fungi and colonization levels of *Gilliamella* per bee gut. **(A)** Total number of bacteria (both *S. alvi* and *Gilliamella*) was determined by plating homogenized guts on BHIA and counting CFUs. Each dot represents a single bee gut and red bars represent the median value for each group. Horizontal dotted line represents LOD = < 70. No colonies were observed in samples plotted below the LOD line. Wilcoxon rank sum test was done with *S. alvi* (Pollen -) as reference group, ns, nonsignificant; ****P < 0.001. (**B**) Bacterial cells (number of bacterial genome equivalents) per bee gut determined by qPCR using genus-specific *Gilliamella* 16S rRNA gene primers. Each dot represents the number of cells in a single bee gut, red bars represent the median, horizontal black line represents qPCR LOD =< 10^4. The presence of pollen in the diet is indicated by (P). Wilcoxon rank sum test was done with *Gilliamella* (Pollen -) as reference group, ns, nonsignificant; ****P < 0.001. (**C**) Number of 16S rRNA gene copies per bee gut and in three different quantities of

677 sterilized bee pollen as determined by qPCR using universal 16S rRNA gene primers. Each dot
678 represents the 16S rRNA gene copies in a single bee gut, red bars represent the median, horizontal black
679 line represents qPCR LOD = < $8x10^3$. The presence of pollen in the diet is indicated by (P). Wilcoxon
680 rank sum test was done with MF (Pollen -) as reference group, ns, nonsignificant; ****P < 0.001. The
681 number of 16S rRNA gene copies detected in DNA extracted from different quantities of sterile pollen
682 used in the bee diet is shown in a separate plot. The high background signal in samples containing pollen
683 comes from the amplification of chloroplast DNA as shown in previous studies [52]. (**D**) Number of 18S
684 rRNA gene copies per bee gut and in three different quantities of sterilized bee pollen as determined by
685 qPCR using universal 18S rRNA gene primers. Each dot represents the 18S rRNA gene copies in a
686 single bee gut, red bars represent the median, horizontal black line represents qPCR LOD = < 10^4. The
687 presence of pollen in the diet is indicated by (P). Wilcoxon rank sum test was done with MF (Pollen -)
688 as reference group, ns, nonsignificant; ****P < 0.001.

689

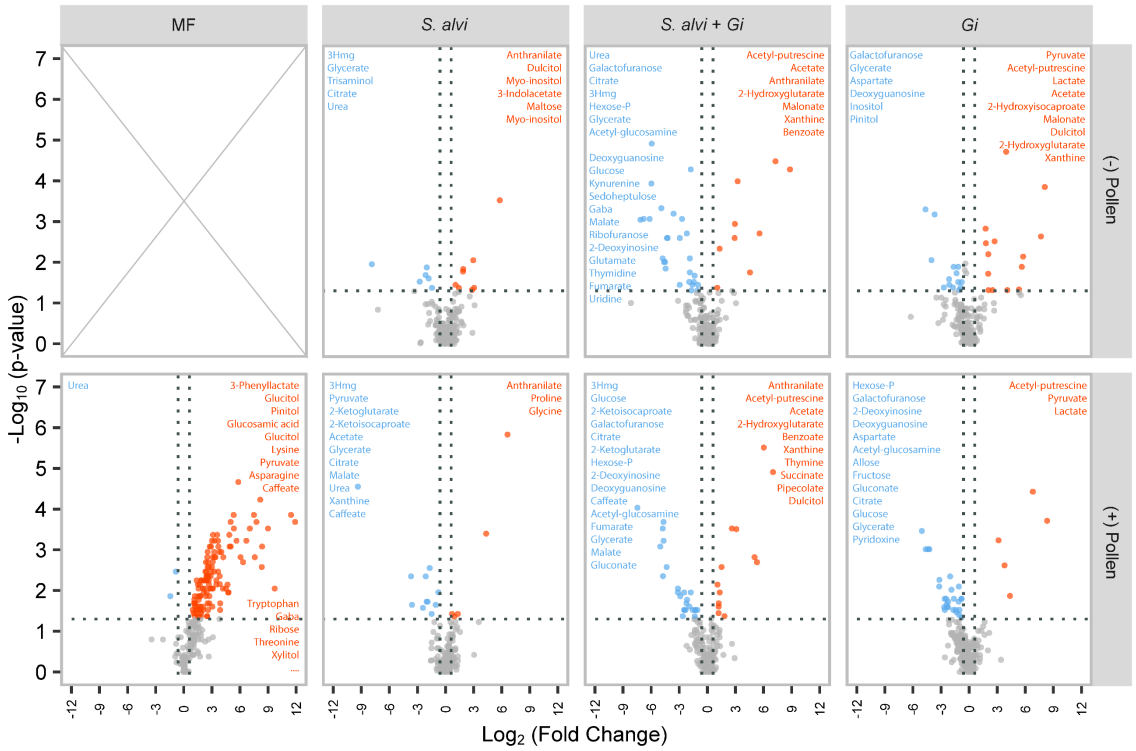

Figure S2. Volcano plots highlighting gut metabolite abundance changes between colonized and microbiota-free (MF) bees with and without pollen. Significantly differentially abundant metabolites between mono- and co-colonized *S. alvi* and *Gilliamella (Gi)* vs MF bees, as well as between MF ((+) Pollen) and MF ((-) Pollen) bees. Significantly depleted and produced metabolites are shown in blue and orange, respectively. Annotations are listed in order of significance for identified metabolites, with isomers and other duplications removed. The full set of significantly more abundant metabolites in the first panel can be found in the supporting scripts. Adjusted significance values were calculated using Wilcoxon rank sum test, and Benjamini-Hochberg correction, using the MF conditions as a reference.

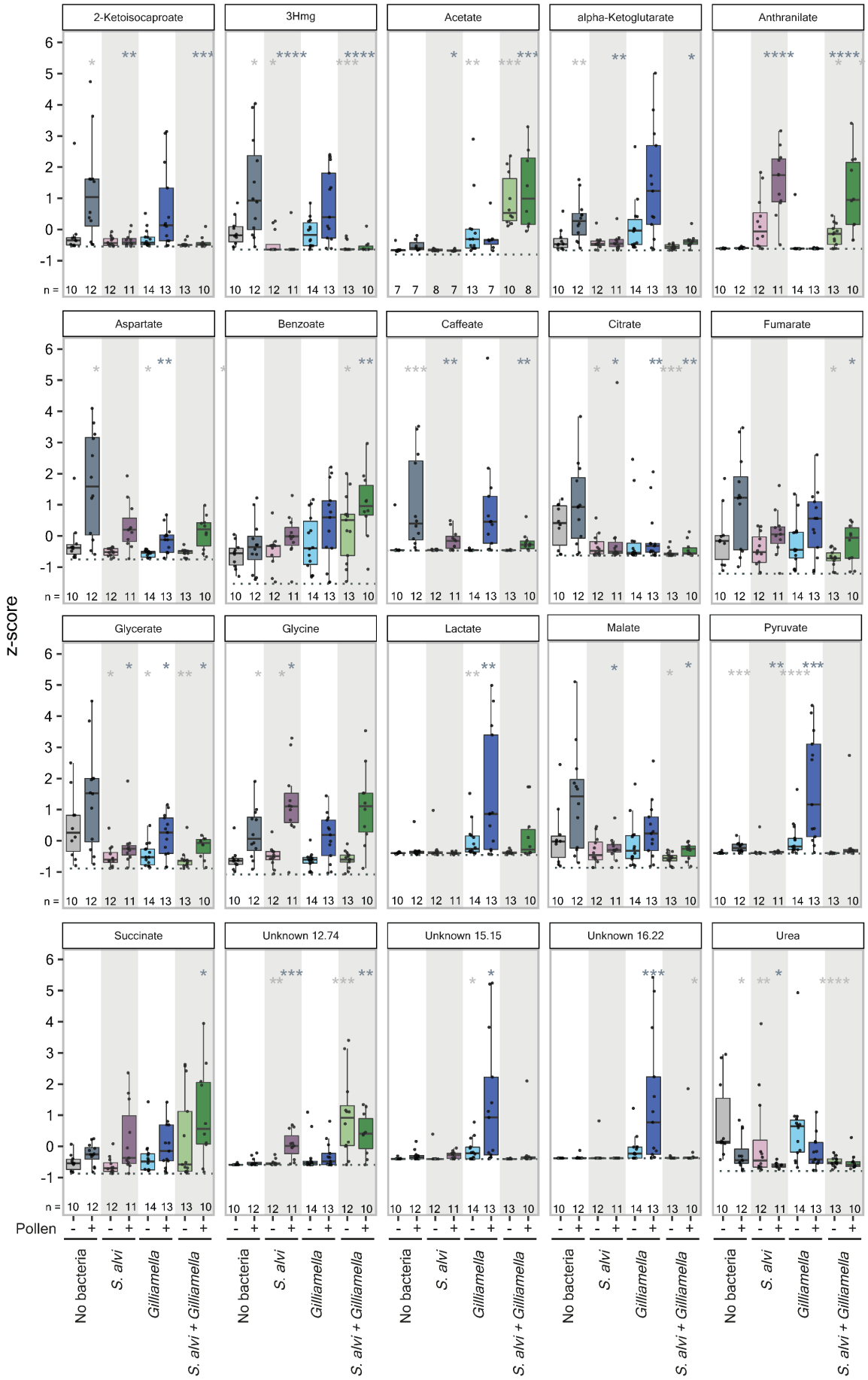
2-Ketoisocaproate
3Hmg
Acetate
alpha-Ketoglutarate
Anthranilate
Aspartate
Benzoate
Caffeate
Citrate
Fumarate
Glycerate
Glycine
Lactate
Malate
Pyruvate
Succinate
Unknown 12.74
Unknown 15.15
Unknown 16.22
Urea
z-score
n =
Pollen
No bacteria
S. alvi
Gilliamella
S. alvi + Gilliamella

700

Figure S3. Z-score normalized metabolite abundances of compounds significantly affected by *S. alvi* colonization. Box plots and individual data points display values across all 8 experimental conditions. Only metabolites in which a mixed linear model showed a significant effect of *S. alvi* colonization are plotted. Multiple types of metabolic interactions are shown. For example, metabolite depletion by *S. alvi* exclusively (2-ketoisocaproate, 3Hmg, caffeate, urea) or by both species (aspartate, citrate, glycerate), metabolite production by *S. alvi* exclusively (anthranilate, unknown 12.74), cross-feeding from *Gilliamella* to *S. alvi* (pyruvate, lactate), synergistic metabolite depletion (fumarate, malate) and production (acetate, benzoate). The light and dark gray asterisks show groups significantly different from MF bees fed sugar water and pollen or only sugar water (also indicated by +/- sign), calculated using Wilcoxon rank sum test, * P < 0.05, ** < 0.01, *** < 0.001, **** < 0.0001. The dotted line represents the transformed LOD for each metabolite.

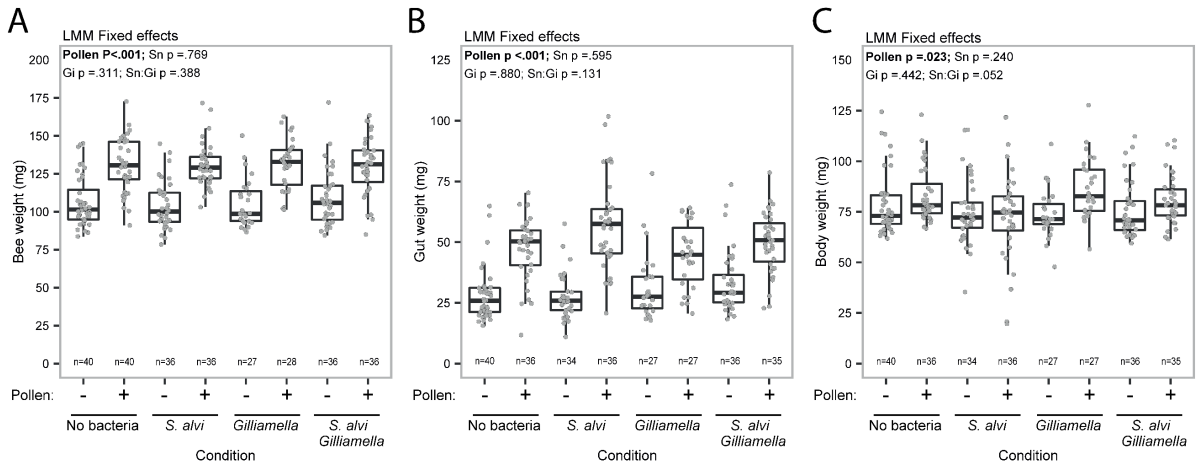

Figure S4. Pollen consumption but not colonization increases bee gut weight. (**A**) Whole bee and (**B**) dissected bee gut weights are strongly influenced by pollen in the diet, but not by colonization treatment. (**C**) The body weight, or difference between bee and gut weights, was also slightly higher across colonization groups for bees fed a pollen diet. The p-values (ANOVA) are shown for the fixed effect terms in the linear mixed models fitted by ML with nested, random cage effects.

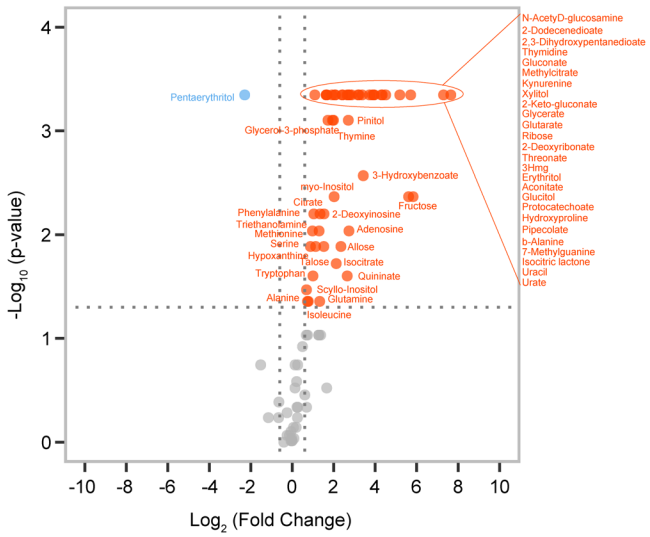

Figure S5. Volcano plot highlighting gut metabolic changes between Day 0 and Day 6 after emergence in MF bees without pollen. Many metabolites are more abundant in the gut on Day 6 than on Day 0 after emergence. Significantly less and more abundant metabolites on Day 6 are shown and annotated in blue and orange, respectively, with isomers and other duplications removed. Adjusted significance values were calculated using Wilcoxon rank sum test, and Benjamini-Hochberg correction, using the day zero conditions as a reference (n=8).

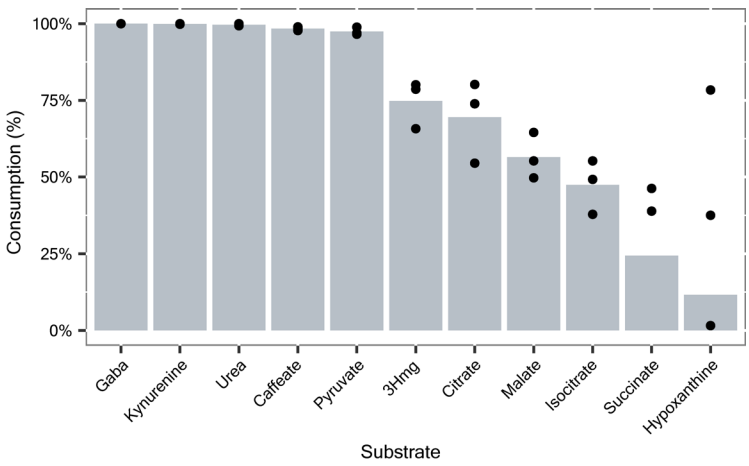

Figure S6. *In vitro* consumption of carbon substrates. The percentage of each carbon source consumed by the end of the *in vitro* growth experiment is shown for each tested carbon source. Data was taken from the condition in which all carbon sources were added to Bee9 media in equimolar amounts. Bars represent the average value from 3 biological replicates (black dots).

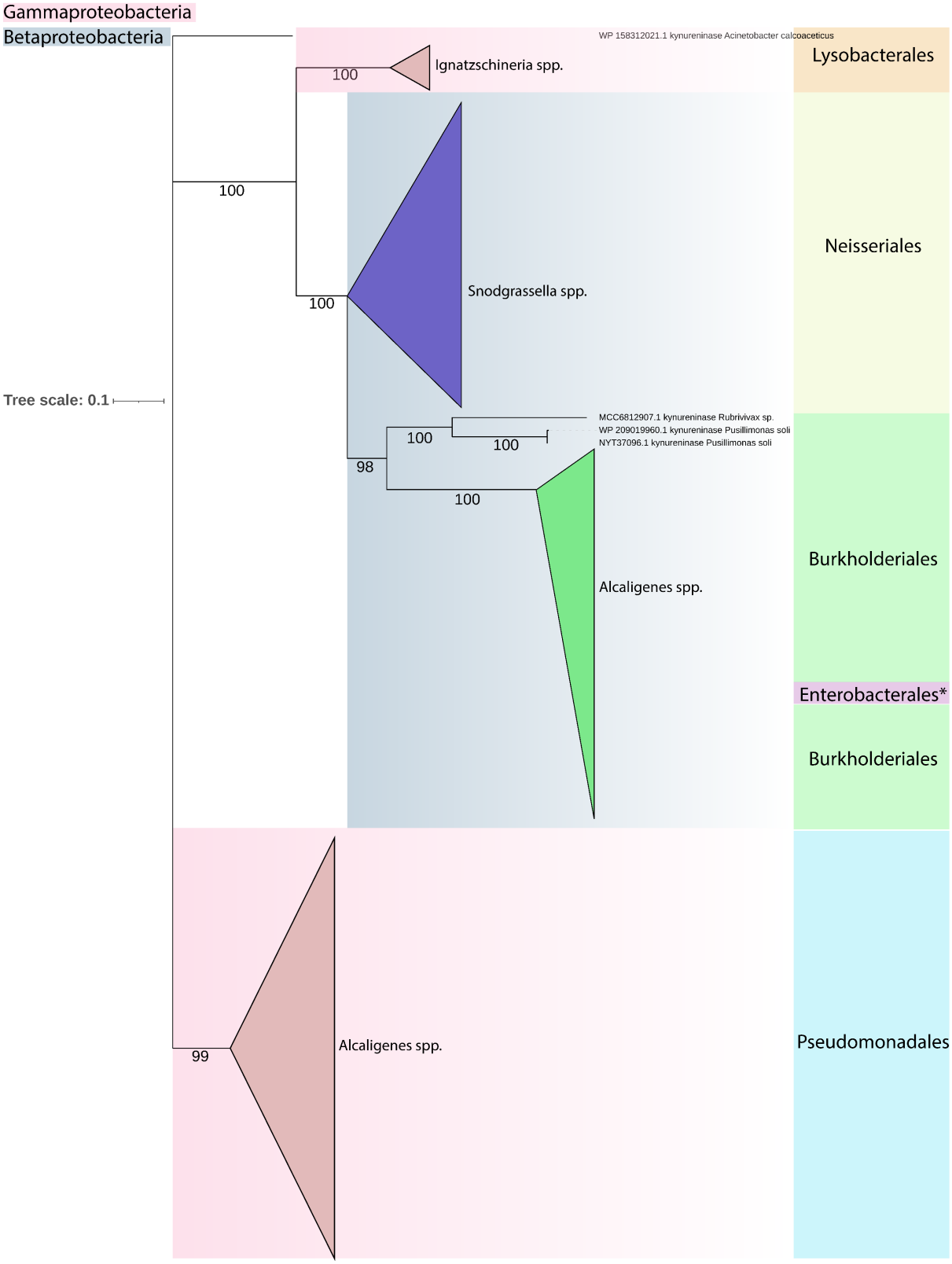

732

733 **Figure S7. Phylogenetic tree of the kynureninase gene family found in *S. alvi*.** The amino acid
734 sequences of 227 homologs of the kynureninase gene identified in *S. alvi* wkb2 were retrieved from
735 NCBI. The tree was inferred with Iqtree after aligning the sequences with MUSCLE (see methods).
736 Tips are collapsed for clades that contain sequences of the same genus. Colored boxes on the right

737 indicate the bacterial family. Bootstrap values are indicated before every node. Gammaproteobacteria
738 are highlighted in pink and Betaproteobacteria in blue. Asterisk indicates a sequence (MBY6345856.1)
739 from Providencia rettgeri, a Gammaproteobacterium, which clusters together with homologs of the
740 kynureninase of Betaproteopbacteria.

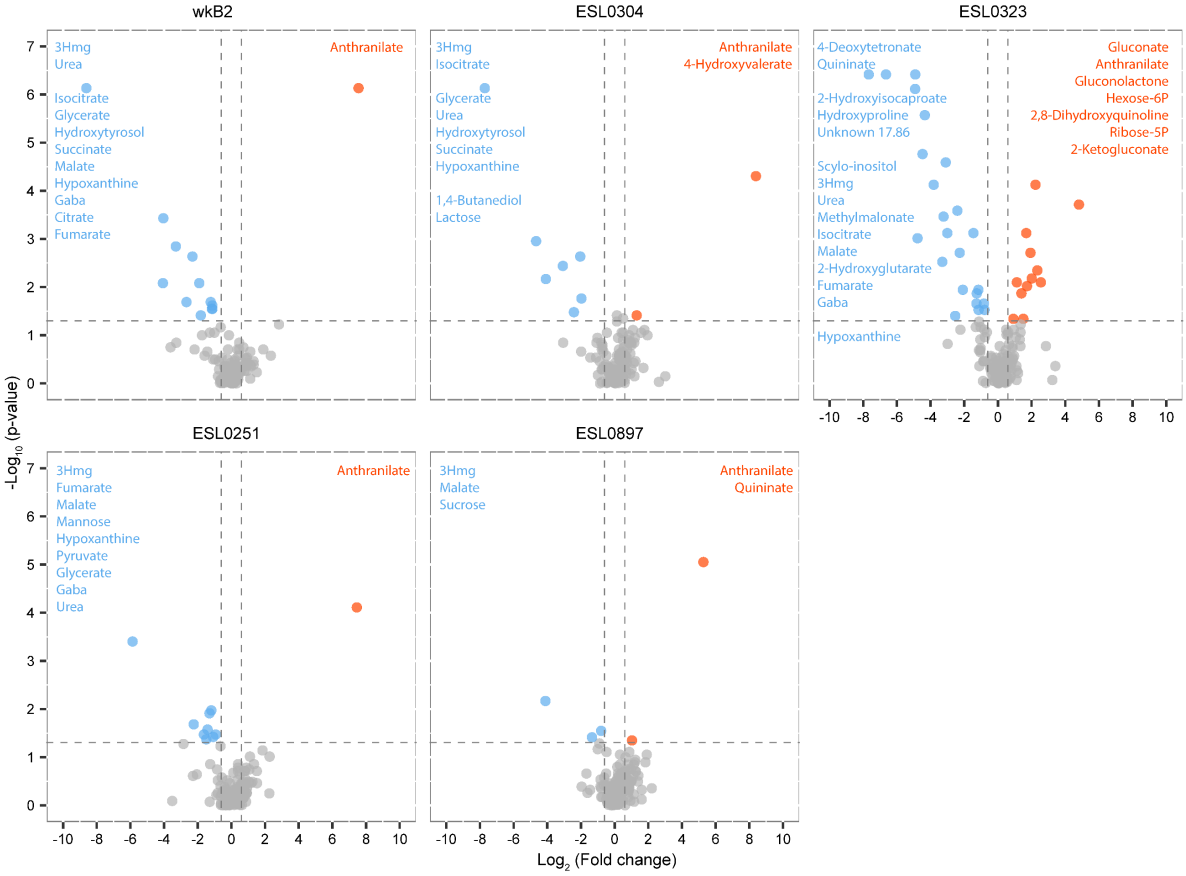

741

742 **Figure S8. Gut metabolite changes in bees mono-colonized with divergent *Snodgrassella* strains**
743 **relative to microbiota-free (MF) bees.** Volcano plot of gut metabolites showing the similarities in
744 metabolite changes from colonized vs MF bees across strains. Top: Strains native to *A. mellifera*;
745 Bottom: Strains native to *Bombus sp.* Significantly depleted and produced metabolites are shown in
746 blue and orange, respectively. Adjusted significance values were calculated using Wilcoxon rank sum
747 test, and Benjamini-Hochberg correction, using the MF condition as a reference.

748

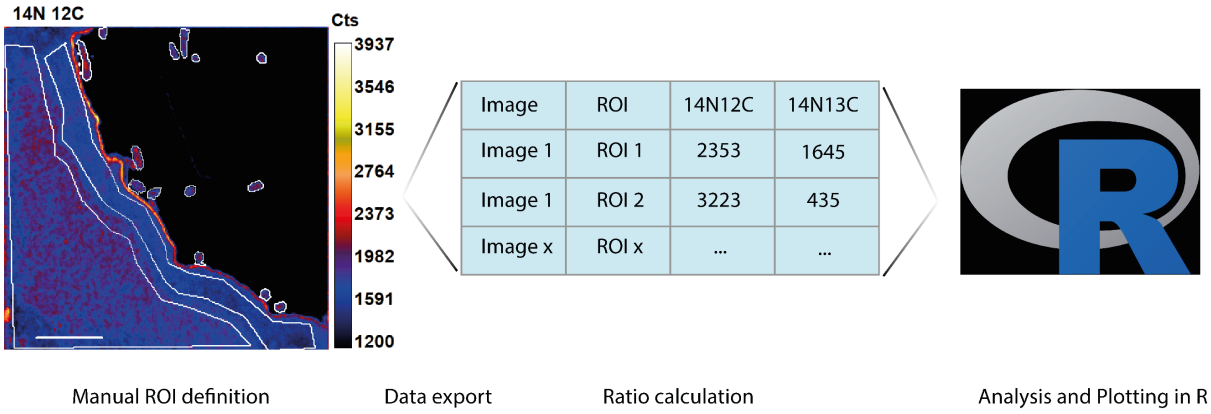

Figure S9. NanoSIMS image analysis workflow. For each image, 10 layers were acquired by bombarding the surface of the samples with Cs+ Ion beam (See methods). The image processing was performed using "L'image" software (Larry Nittler, Carnegie Institution of Washington). The 10 layers were aligned and stacked and 44 ms deadtime correction was applied. Regions of interests (ROI) were manually drawn around bacterial cells, gut epithelium layer, and bulk host cells, using a minimum threshold specified and values were extracted and reported in **Dataset S1**. At% enrichment was calculated in R using the data.table package. At% enrichment formula: $13C\ At\% = {}^{14N\ 13C}/_{(14N\ 13C\ +\ 14N\ 12C)} \times 100.$

759 **Table S1. Bacterial strains used in this study.** [12,53,54]

Bacterial strain	# 16S rRNA copies	Culturing condition	Strain source	Place of origin
Gilliamella apicola wkB1^{T}	4	BHIA, 35°C, microaerophilic	(Kwong & Moran, 2013)	New Haven, USA
Gilliamella apis ESL0169	4	BHIA, 35°C, microaerophilic	(Kešnerová et al., 2017)	Lausanne, Switzerland
Gilliamella sp. ESL0182	4	BHIA, 35°C, microaerophilic	(Ellegaard & Engel, 2018)	Lausanne, Switzerland
Gilliamella apis ESL0297	4	BHIA, 35°C, microaerophilic	This study	Lausanne, Switzerland
Snodgrassella alvi wkB2^{T}	4	TSA, 35°C, microaerophilic	(Kwong & Moran, 2013)	New Haven, USA
Snodgrassella alvi ESL0304	4	TSA, 35°C, microaerophilic	This study	Lausanne, Switzerland
Snodgrassella alvi ESL0323	4	TSA, 35°C, microaerophilic	This study	Lausanne, Switzerland
Snodgrassella alvi ESL0251	4	TSA, 35°C, microaerophilic	This study	Lausanne, Switzerland
Snodgrassella alvi ESL0897	4	TSA, 35°C, microaerophilic	This study	Lausanne, Switzerland

760

761

762 **Table S2. *S. alvi* & *Gilliamella* colonization summary counts.** Total bee numbers per experiment,
763 survival rate, number of bees used for CFU plating, qPCR and metabolomics analysis, and pollen
764 consumption are shown.

	Replicate	1	2	3	4	5	Total
Bees	MD	34	24	24	24	0	106
	MD (P)	30	23	23	25	0	101
	Sn	31	24	20	0	20	95
	Sn (P)	34	23	20	0	19	96
	Sn+Gi	32	22	24	0	16	94
	Sn+Gi (P)	29	24	20	0	22	95
	Gi	0	0	0	26	25	51
	Gi (P)	0	0	0	25	25	50
Survival (%)	MD	100%	100%	100%	96%	N/A	99%
	MD (P)	100%	100%	100%	100%	N/A	100%
	Sn	94%	100%	100%	N/A	100%	98%
	Sn (P)	100%	100%	95%	N/A	100%	99%
	Sn+Gi	97%	95%	100%	N/A	100%	98%
	Sn+Gi (P)	97%	92%	95%	N/A	100%	96%
	Gi	N/A	N/A	N/A	100%	100%	100%
	Gi (P)	N/A	N/A	N/A	96%	100%	98%
CFU	MD	10	10	10	10	N/A	40
	MD (P)	10	10	10	10	N/A	40
	Sn	10	10	10	N/A	6	36
	Sn (P)	10	10	10	N/A	6	36
	Sn+Gi	10	10	10	N/A	6	36
	Sn+Gi (P)	10	10	10	N/A	6	36
	Gi	N/A	N/A	N/A	10	18	28
	Gi (P)	N/A	N/A	N/A	10	18	28
qPCR	MD	4	3	4	6	N/A	17
	MD (P)	4	3	4	5	N/A	16
	Sn	4	9	6	N/A	6	25
	Sn (P)	4	9	8	N/A	6	27
	Sn/Gi	10	10	11	N/A	6	37
	Sn/Gi (P)	10	10	10	N/A	6	36
	Gi	N/A	N/A	N/A	10	14	24
	Gi (P)	N/A	N/A	N/A	9	21	30
Metabolomics	MD	2	1	2	5	N/A	10
	MD (P)	2	1	4	5	N/A	12
	Sn	1	1	2	N/A	6	10
	Sn (P)	1	1	3	N/A	6	11
	Sn+Gi	3	1	5	N/A	6	15
	Sn+Gi (P)	1	1	4	N/A	5	11
	Gi	N/A	N/A	N/A	5	9	14
	Gi (P)	N/A	N/A	N/A	6	7	13
Pollen Consumption (mg/bee)	MD	-	-	-	-	-	-
	MD (P)	30	33	32	13	N/A	26
	Sn	-	-	-	-	-	-
	Sn (P)	20	31	30	N/A	22	26
	Sn+Gi	-	-	-	-	-	-
	Sn+Gi (P)	19	30	33	N/A	16	24
	Gi	-	-	-	-	-	-
	Gi (P)	N/A	N/A	N/A	17	18	17

765

766 **Table S3. Summary of the number of bees sampled per replicate and treatment for the mono-**

767 **colonization experiment with divergent *Snodgrassella* strains.** Total number of bees per experiment,

768 survival rate, and number of bees used for CFU plating and metabolomics analysis are shown.

	Replicate	1	2	Total
Bees	MD	14	15	29
	wkB2	14	14	28
	251	16	15	31
	304	14	15	29
	323	14	15	29
	892	14	15	29
	897	15	14	29
Survival (%)	MD	93%	100%	96%
	wkB2	100%	100%	100%
	251	88%	100%	94%
	304	100%	80%	90%
	323	100%	100%	100%
	892	86%	100%	93%
	897	80%	79%	79%
CFU	MD	12	12	24
	wkB2	12	12	24
	251	11	12	23
	304	12	9	21
	323	12	12	24
	892	12	12	24
	897	12	9	21
Metabolomics	MD	6	6	12
	wkB2	6	6	12
	251	8	9	17
	304	6	6	12
	323	7	6	13
	892	6	6	12
	897	6	6	12

769

References

1 Tremaroli, V. & Bäckhed, F. Functional interactions between the gut microbiota and host metabolism. *Nature* **489**, 242-249, doi:10.1038/nature11552 (2012).

2 Kwong, W. K. & Moran, N. A. Gut microbial communities of social bees. *Nature Reviews Microbiology* **14**, 374-384, doi:10.1038/nrmicro.2016.43 (2016).

3 Bonilla-Rosso, G. & Engel, P. Functional roles and metabolic niches in the honey bee gut microbiota. *Current Opinion in Microbiology* **43**, 69-76, doi:10.1016/j.mib.2017.12.009 (2018).

4 Kwong, W. K. *et al.* Dynamic microbiome evolution in social bees. *Science Advances* **3**, e1600513, doi:10.1126/sciadv.1600513 (2017).

5 Li, Y., Leonard, S. P., Powell, J. E. & Moran, N. A. Species divergence in gut-restricted bacteria of social bees. *Proceedings of the National Academy of Sciences* **119**, e2115013119, doi:10.1073/pnas.2115013119 (2022).

6 Wu, J. *et al.* Honey bee genetics shape the strain-level structure of gut microbiota in social transmission. *Microbiome* **9**, 225, doi:10.1186/s40168-021-01174-y (2021).

7 Engel, P. *et al.* Standard methods for research on Apis mellifera gut symbionts. *Journal of Apicultural Research* **52**, 1-24, doi:10.3896/ibra.1.52.4.07 (2013).

8 Ricigliano, V. A. & Anderson, K. E. Probing the Honey Bee Diet-Microbiota-Host Axis Using Pollen Restriction and Organic Acid Feeding. *Insects* **11**, 291, doi:10.3390/insects11050291 (2020).

9 Zheng, H., Steele, M. I., Leonard, S. P., Motta, E. V. S. & Moran, N. A. Honey bees as models for gut microbiota research. *Lab Animal* **47**, 317-325, doi:10.1038/s41684-018-0173-x (2018).

10 Kwong, W. K., Engel, P., Koch, H. & Moran, N. A. Genomics and host specialization of honey bee and bumble bee gut symbionts. *Proceedings of the National Academy of Sciences* **111**, 11509-11514, doi:doi:10.1073/pnas.1405838111 (2014).

11 Martinson, V. G., Moy, J. & Moran, N. A. Establishment of characteristic gut bacteria during development of the honeybee worker. *Appl Environ Microbiol* **78**, 2830-2840, doi:10.1128/aem.07810-11 (2012).

12 Kešnerová, L. *et al.* Disentangling metabolic functions of bacteria in the honey bee gut. *PLOS Biology* **15**, e2003467, doi:10.1371/journal.pbio.2003467 (2017).

13 Schwartzman, J. A. *et al.* The chemistry of negotiation: Rhythmic, glycan-driven acidification in a symbiotic conversation. *Proceedings of the National Academy of Sciences* **112**, 566-571, doi:10.1073/pnas.1418580112 (2015).

14 Desai, M. S. *et al.* A Dietary Fiber-Deprived Gut Microbiota Degrades the Colonic Mucus Barrier and Enhances Pathogen Susceptibility. *Cell* **167**, 1339-1353.e1321, doi:https://doi.org/10.1016/j.cell.2016.10.043 (2016).

15 Sonnenburg, J. L. *et al.* Glycan Foraging in Vivo by an Intestine-Adapted Bacterial Symbiont. *Science* **307**, 1955-1959, doi:10.1126/science.1109051 (2005).

16 Berry, D. *et al.* Host-compound foraging by intestinal microbiota revealed by single-cell stable isotope probing. *Proceedings of the National Academy of Sciences* **110**, 4720-4725, doi:10.1073/pnas.1219247110 (2013).

17 Sicard, J.-F., Le Bihan, G., Vogeleer, P., Jacques, M. & Harel, J. Interactions of Intestinal Bacteria with Components of the Intestinal Mucus. *Frontiers in Cellular and Infection Microbiology* **7**, doi:10.3389/fcimb.2017.00387 (2017).

18 Martens, E. C., Chiang, H. C. & Gordon, J. I. Mucosal Glycan Foraging Enhances Fitness and Transmission of a Saccharolytic Human Gut Bacterial Symbiont. *Cell Host & Microbe* **4**, 447-457, doi:10.1016/j.chom.2008.09.007 (2008).

19 Miyashiro, T. *et al.* The N-acetyl-d-glucosamine repressor NagC of Vibrio fischeri facilitates colonization of Euprymna scolopes. *Molecular Microbiology* **82**, 894-903, doi:https://doi.org/10.1111/j.1365-2958.2011.07858.x (2011).

20 Wier, A. M. *et al.* Transcriptional patterns in both host and bacterium underlie a daily rhythm of anatomical and metabolic change in a beneficial symbiosis. *Proceedings of the National Academy of Sciences* **107**, 2259-2264, doi:10.1073/pnas.0909712107 (2010).
21 Zeng, X. *et al.* Gut bacterial nutrient preferences quantified *in vivo*. *Cell* **185**, 3441-3456.e3419, doi:10.1016/j.cell.2022.07.020 (2022).
22 Gillis, C. C. *et al.* Dysbiosis-Associated Change in Host Metabolism Generates Lactate to Support Salmonella Growth. *Cell Host & Microbe* **23**, 54-64.e56, doi:https://doi.org/10.1016/j.chom.2017.11.006 (2018).
23 Rosenberg, G. *et al.* Host succinate is an activation signal for *Salmonella* virulence during intracellular infection. *Science* **371**, 400-405, doi:10.1126/science.aba8026 (2021).
24 Nguyen, B. D. *et al.* Import of Aspartate and Malate by DcuABC Drives H2/Fumarate Respiration to Promote Initial Salmonella Gut-Lumen Colonization in Mice. *Cell Host & Microbe* **27**, 922-936.e926, doi:10.1016/j.chom.2020.04.013 (2020).
25 Zheng, H., Powell, J. E., Steele, M. I., Dietrich, C. & Moran, N. A. Honeybee gut microbiota promotes host weight gain via bacterial metabolism and hormonal signaling. *Proceedings of the National Academy of Sciences* **114**, 4775-4780, doi:10.1073/pnas.1701819114 (2017).
26 Brochet, S. *et al.* Niche partitioning facilitates coexistence of closely related honey bee gut bacteria. *eLife* **10**, doi:10.7554/elife.68583 (2021).
27 Powell, J. E., Leonard, S. P., Kwong, W. K., Engel, P. & Moran, N. A. Genome-wide screen identifies host colonization determinants in a bacterial gut symbiont. *Proceedings of the National Academy of Sciences* **113**, 13887-13892, doi:10.1073/pnas.1610856113 (2016).
28 Kwong, W. K., Zheng, H. & Moran, N. A. Convergent evolution of a modified, acetate-driven TCA cycle in bacteria. *Nature Microbiology* **2**, 17067, doi:10.1038/nmicrobiol.2017.67 (2017).
29 Sharp, C. & Foster, K. R. Host control and the evolution of cooperation in host microbiomes. *Nature Communications* **13**, 3567, doi:10.1038/s41467-022-30971-8 (2022).
30 Steele, M. I., Motta, E. V. S., Gattu, T., Martinez, D. & Moran, N. A. The Gut Microbiota Protects Bees from Invasion by a Bacterial Pathogen. *Microbiology Spectrum* **9**, e00394-00321, doi:10.1128/Spectrum.00394-21 (2021).
31 Feng, Y. *et al.* Anopheline mosquitoes are protected against parasite infection by tryptophan catabolism in gut microbiota. *Nature Microbiology* **7**, 707-715, doi:10.1038/s41564-022-01099-8 (2022).
32 Cerstiaens, A. *et al.* Neurotoxic and neurobehavioral effects of kynurenines in adult insects. *Biochemical and Biophysical Research Communications* **312**, 1171-1177, doi:https://doi.org/10.1016/j.bbrc.2003.11.051 (2003).
33 Marszalek-Grabska, M. *et al.* Kynurenine emerges from the shadows – Current knowledge on its fate and function. *Pharmacology & Therapeutics* **225**, 107845, doi:https://doi.org/10.1016/j.pharmthera.2021.107845 (2021).
34 Schwarcz, R. & Stone, T. W. The kynurenine pathway and the brain: Challenges, controversies and promises. *Neuropharmacology* **112**, 237-247, doi:https://doi.org/10.1016/j.neuropharm.2016.08.003 (2017).
35 Scheiner, R., Baumann, A. & Blenau, W. Aminergic control and modulation of honeybee behaviour. *Curr Neuropharmacol* **4**, 259-276, doi:10.2174/157015906778520791 (2006).
36 Zhang, Z. *et al.* Honeybee gut Lactobacillus modulates host learning and memory behaviors via regulating tryptophan metabolism. *Nature Communications* **13**, 2037, doi:10.1038/s41467-022-29760-0 (2022).
37 Hu, Y. *et al.* Herbivorous turtle ants obtain essential nutrients from a conserved nitrogen-recycling gut microbiome. *Nature Communications* **9**, 964, doi:10.1038/s41467-018-03357-y (2018).
38 Kešnerová, L. *et al.* Gut microbiota structure differs between honeybees in winter and summer. *The ISME Journal* **14**, 801-814, doi:10.1038/s41396-019-0568-8 (2020).
39 Nocelli, R. C., Cintra-Socolowski, P., Roat, T. C., Silva-Zacarin, E. C. M. & Malaspina, O.
40 Yagi, S. & Ogawa, H. Effect of Tryptophan Metabolites on Fluorescent Granules in the Malpighian Tubules of Eye Color Mutants of *Drosophila melanogaster*. *Zoological Science* **13**, 97-104, 108 (1996).

41 Emery, O., Schmidt, K. & Engel, P. Immune system stimulation by the gut symbiont *Frischella perrara* in the honey bee (*Apis mellifera*). *Molecular Ecology* **26**, 2576-2590, doi:https://doi.org/10.1111/mec.14058 (2017).

42 Tauber, J. P. *et al.* Honeybee intestines retain low yeast titers, but no bacterial mutualists, at emergence. *Yeast* **39**, 95-107, doi:https://doi.org/10.1002/yea.3665 (2022).

43 den Besten, G. *et al.* The Short-Chain Fatty Acid Uptake Fluxes by Mice on a Guar Gum Supplemented Diet Associate with Amelioration of Major Biomarkers of the Metabolic Syndrome. *PLOS ONE* **9**, e107392, doi:10.1371/journal.pone.0107392 (2014).

44 Fiehn, O. *et al.* Quality control for plant metabolomics: reporting MSI-compliant studies. *The Plant Journal* **53**, 691-704, doi:10.1111/j.1365-313x.2007.03387.x (2008).

45 Wanichthanarak, K., Jeamsripong, S., Pornputtapong, N. & Khoomrung, S. Accounting for biological variation with linear mixed-effects modelling improves the quality of clinical metabolomics data. *Computational and Structural Biotechnology Journal* **17**, 611-618, doi:https://doi.org/10.1016/j.csbj.2019.04.009 (2019).

46 Nargund, S., Misra, A., Zhang, X., Coleman, G. D. & Sriram, G. Flux and reflux: metabolite reflux in plant suspension cells and its implications for isotope-assisted metabolic flux analysis. *Molecular BioSystems* **10**, 1496-1508, doi:10.1039/C3MB70348G (2014).

47 Rosenblatt, J., Chinkes, D., Wolfe, M. & Wolfe, R. R. Stable isotope tracer analysis by GC-MS, including quantification of isotopomer effects. *American Journal of Physiology-Endocrinology and Metabolism* **263**, E584-E596, doi:10.1152/ajpendo.1992.263.3.E584 (1992).

48 Kremer, J. R., Mastronarde, D. N. & McIntosh, J. R. Computer Visualization of Three-Dimensional Image Data Using IMOD. *Journal of Structural Biology* **116**, 71-76, doi:https://doi.org/10.1006/jsbi.1996.0013 (1996).

49 Hoppe, P., Cohen, S. & Meibom, A. NanoSIMS: Technical Aspects and Applications in Cosmochemistry and Biological Geochemistry. *Geostandards and Geoanalytical Research* **37**, 111-154, doi:https://doi.org/10.1111/j.1751-908X.2013.00239.x (2013).

50 Edgar, R. C. MUSCLE: multiple sequence alignment with high accuracy and high throughput. *Nucleic Acids Res* **32**, 1792-1797, doi:10.1093/nar/gkh340 (2004).

51 Nguyen, L. T., Schmidt, H. A., von Haeseler, A. & Minh, B. Q. IQ-TREE: a fast and effective stochastic algorithm for estimating maximum-likelihood phylogenies. *Mol Biol Evol* **32**, 268-274, doi:10.1093/molbev/msu300 (2015).

52 Moran, N. A., Hansen, A. K., Powell, J. E. & Sabree, Z. L. Distinctive Gut Microbiota of Honey Bees Assessed Using Deep Sampling from Individual Worker Bees. *PLOS ONE* **7**, e36393, doi:10.1371/journal.pone.0036393 (2012).

53 Kwong, W. K. & Moran, N. A. Cultivation and characterization of the gut symbionts of honey bees and bumble bees: description of *Snodgrassella alvi* gen. nov., sp. nov., a member of the family *Neisseriaceae* of the. *International Journal of Systematic and Evolutionary Microbiology* **63**, 2008-2018, doi:10.1099/ijs.0.044875-0 (2013).

54 Ellegaard, K. M. & Engel, P. New Reference Genome Sequences for 17 Bacterial Strains of the Honey Bee Gut Microbiota. *Microbiol Resour Announc* **7**, doi:10.1128/mra.00834-18 (2018).